ADVANCED FUNCTIONAL MATERIALS

Porous Chromium Terephthalate MIL-101 with Coordinatively Unsaturated Sites: Surface Functionalization, Encapsulation, Sorption and Catalysis

By *Do-Young Hong, Young Kyu Hwang,* Christian Serre, Gérard Férey,* and *Jong-San Chang**

A metal–organic framework (MOF), chromium(III) terephthalate (MIL-101), possesses several unprecedented features such as a mesoporous zeotype architecture with mesoporous cages and microporous windows, a giant cell volume, huge surface area, and numerous unsaturated chromium sites. The presence of unsaturated Cr(III) sites in MIL-101 provides an intrinsic chelating property with electron-rich functional groups. This feature offers a powerful way to selectively functionalize the unsaturated sites in the MOFs, differing in many respects from the functionalization of mesoporous silica and other porous hybrids reported so far. This work demonstrates that the surface amine-grafting undoubtedly provides a general way of selective functionalization of porous MOFs besides that with unsaturated metal sites. The present approach indeed ensures the development of functionalized MOFs for the immobilization and encapsulation of organic molecules and metal components that are useful for catalysis, adsorption, molecular recognition, and so on. Here some of the recent ideas concerning site-selective functionalization of MIL-101 are examined and explained, focusing on the utilization of unsaturated Cr(III) sites. Recent advances in synthesis, selective surface functionalization, outstanding sorption properties, encapsulation of nano-objects, and catalytic applications in MIL-101 are also described.

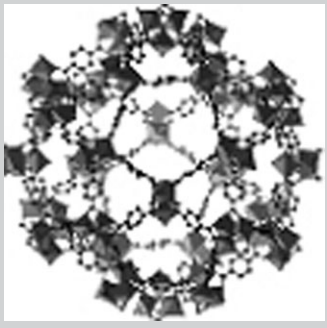

1. Introduction

Crystalline aluminosilicate zeolites with tetrahedral frameworks have been used widely in the domains of separations, ion exchange, and shape-selective catalysis.[1–4] However, much effort to discover a new type of crystalline nanoporous materials has been continuously tried in order to overcome drawbacks of conventional zeolites such as limited incorporation of metal element and limited pore sizes to induce diffusion problem.[5] As a result, there has been a tremendous increase in the synthesis of non-aluminosilicate-based crystalline porous materials during the past decade (Fig. 1).[6–13] Nowadays, there has been an enormous growth in the chemical diversity of crystalline nanoporous materials in new compositional domains. Among them, porous hybrid materials with crystallized metal–organic frameworks (MOFs) are currently of great interest and importance[14–19] due to their novel co-ordination structures, diverse topologies, and potential applications in gas storage,[20–29] separation,[30,31] catalysis,[32–37] drug delivery,[38,39] molecular recognition,[40] luminescence,[41–43] magnetism,[44,45] and conductivity.[46] Basically, MOFs result from the tight association and three-dimensional (3D) covalent connection of inorganic clusters and organic moieties to build up open frameworks.[47] Conceptually, there is almost no difference between classical inorganic porous materials and hybrid ones; for example, the 3D skeleton can be described for both of them by the association of secondary building units (SBUs). In the SBUs of MOFs, the anionic species are replaced by organic linkers, creating a contrast between the bonds within the framework: mainly covalent for the organic parts and ionocovalent for the inorganic.[14] Moreover, the properties of MOFs often resemble those of classical zeolites; for example, they can adsorb gases and allow shape-selective catalysis. However, these MOF materials offer a wider range of structures and properties such as crystallinity, permanent porosity, dynamic porous properties, and functionality of metal ions and organic ligands besides their pivotal features such as designability, regularity, and structural flexibility.[48] Some of them are incredibly light and so porous that the surface area of one gram could cover an entire football or basketball pitch.[49] It may also be possible to make hybrids with properties that are rare in purely organic or inorganic systems.[50]

[*] Dr. J.-S. Chang, Y. K. Hwang, Dr. D.-Y. Hong
Catalysis Center for Molecular Engineering (CCME)
Korea Research Institute of Chemical Technology (KRICT)
P.O. Box, 107, Yusung, Daejeon 305-600 (Korea)
E-mail: jschang@krict.re.kr; ykhwang@krict.re.kr
Dr. C. Serre, Prof. G. Férey
Institut Lavoisier (UMR CNRS 8180)
Université de Versailles Saint Quentin
45 avenue des Etats-Unis
78035 Versailles Cedex (France)

DOI: 10.1002/adfm.200801130

However, a main drawback of MOFs is the weak thermal stability generally limited to 350–400°C, which rules out any application at high temperatures.[14]

By the way, the search for very large pores as well as hierarchical pore structures[51] represents the last challenge in the development of MOFs due to their potential applications. As such, some of us have recently initiated a global study of the trivalent metal carboxylate systems, which has led to the discovery of the chromium(III) carboxylate with giant pores labeled MIL-101 (MIL for materials of institut Lavoisier).[51,52] This hybrid solid is basically built up from a hybrid superterahedral (ST) building unit, which is formed by rigid terephthalate ligands and trimeric chromium(III) octahedral clusters. The resulting cell volume of MIL-101 is very huge (≈702 000 Å^3) with two types of quasi-spherical cages limited by 12 pentagonal faces for the smaller and by 16 faces (12 pentagonal and 4 hexagonal) for the larger.

MIL-101 is one of the most porous materials to date,[24,52,53] being a very prominent example among the many MOFs that have been studied.[54] In this account, we attempt to integrate recent work on MIL-101 mainly performed by the present authors. The aim of this contribution is to describe synthesis, selective surface functionalization, outstanding sorption properties, encapsulation of nano-objects, and catalytic applications in MIL-101

2. Structural Characteristics

Ferey and co-workers initially introduced the concept of ''scale chemistry'',[55] in which the size of the SBUs in a structure is increased while maintaining the same connectivity between them; the larger the SBU, the larger the pores. Recently, they have succeeded in the discovery of novel MOFs, cubic chromium carboxylates MIL-100 and MIL-101 by using the concept. They were actually obtained by the combination of targeted chemistry[56] and computational design of crystal structures.[57]

In particular, MIL-101 was made from the linkage of 1,4-benzene dicarboxylate (BDC) anions and inorganic trimers (Fig. 2a) that consist of three chromium atoms in an octahedral environment with four oxygen atoms of the bidendate dicarboxylates, one μ_3O atom, and one oxygen atom from the terminal water or fluorine group. Octahedra are related through the μ_3O oxygen atom to form the trimeric building unit. A ST building unit is formed by rigid terephthalate ligands and trimeric chromium(III) octahedral clusters. The four vertices of the ST are occupied by the trimers, and the organic linkers are located at the six edges of the ST (Fig. 2b). The size of the ST requires an expansion of the cubic unit cell (space group F d-$3m$) to more than 85 Å before the construction process. The connection between the ST is established through vertices to ensure a 3D network of ''corner sharing'' supertetrahedra with an augmented MTN zeotype architecture derived from the high-silica zeolite ZSM-39[58] (Fig. 2c) and illustrates the concept of scale chemistry.[55] The STs are microporous (with a ≈8.6 Å free aperture for the windows), and the resulting framework delimits two types of mesoporous cages filled with guest molecules. These two cages, which are present in a 2:1 ratio, are delimited by 20 and 28 ST with internal free diameters of ≈29 Å and 34 Å, respectively (Fig. 2d,e). These values correspond to accessible pore volumes of ≈12,700 Å^3 and ≈20,600 Å^3, respectively. The large windows of both cages make the latter accessible to very large molecules. The smaller cages exhibit pentagonal windows with a free opening of ≈12 Å, while the larger cages possess both pentagonal and larger hexagonal windows with a ≈14.5 Å by 16 Å free aperture. Its cubic structure ($a < 89$ Å) exhibits several unprecedented features: a mesoporous zeotype architecture with a MTN topology, a giant cell volume (702 000 Å^3), a large free aperture (12 Å from pentagonal windows and 16 Å × 14.5 Å from hexagonal window), mesoporous cages (29 Å and 34 Å), huge BET and Langmuir surface areas (4100 ± 200 m^2 g^{-1}; 5900 ± 300 m^2 g^{-1}), and numerous unsaturated chromium sites (up to theoretically approximately 3.0 mmol g^{-1}).

As shown in scanning electron microscopy (SEM) image, the dimensions of the MIL-101 crystals range from 0.1 up to 0.4 μm (Fig. 3a). The cubic symmetry of the MIL-101 is reflected in the shape of the crystals. Lebedev et al. reported the first direct imaging of giant pores of MIL-101 with high-resolution transmission electron microscopy (HRTEM).[59] Figure 3b illustrates the HRTEM image of MIL-101 along one major direction [111], showing a perfect hexagonal packing of bright dots

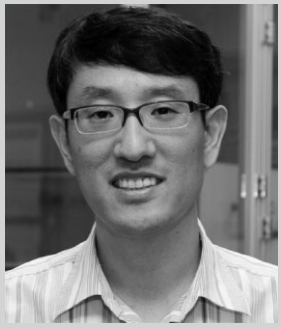

Jong-San Chang is a principal investigator at the Korea Research Institute of Chemical Technology (KRICT). He joined the faculty there in 1988. Previous to that he obtained his B.Sc. degree (1986) from Seoul National University, and MS (1988) and Ph.D. (1996) from the Korea Advanced Institute of Science and Technology. He has been working for KRICT since 1988 and is currently a director of the Research Center for Nanocatalysts. In 1999 he spent a sabbatical period at the Materials Research Laboratory, University of California, Santa Barbara (US) with Prof. A. K. Cheetham. He has been engaged in the fields of zeolite catalysis, energy-related catalysis, and green chemistry. Besides these areas, his present interests cover microwave synthesis, characterization, and applications of nanoporous materials including MOFs.

Young Kyu Hwang is a principal researcher at the Korea Research Institute of Chemical Technology (KRICT). He joined there in 2003. He received his B.Sc., MS, and Ph.D. degrees in 1995, 1997, and 2003, respectively, in chemistry from Sung Kyun Kwan University. In 2000, he worked at the Department of Chemistry at the University of California Santa Barbara US, as a visiting scientist. His present research areas include sol–gel chemistry, microwave synthesis, catalysis, and gas sorption based on new types of nanoporous materials including zeolites, mesoprous materials, MOFs, and organic–inorganic hybrids.

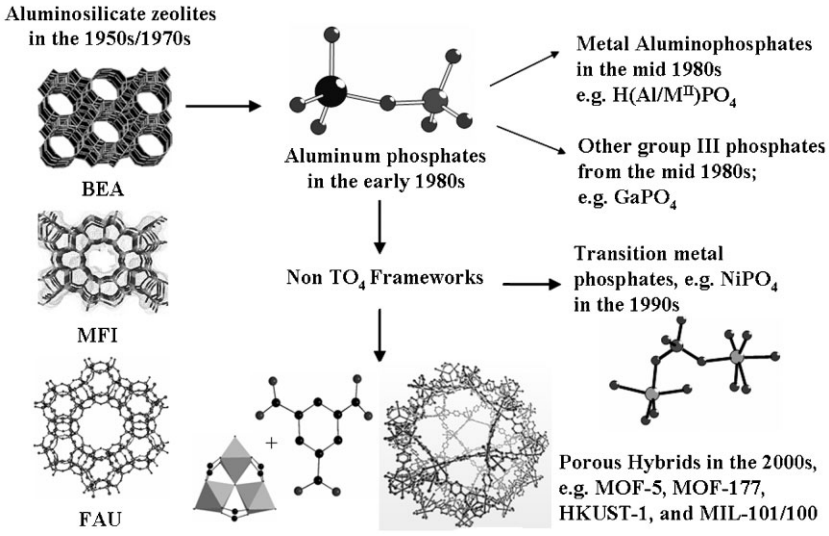

Figure 1. Evolution history of crystalline microporous materials. The 15th International Zeolite Conference (IZC) held in 2007 was entitled ''From Zeolites to Porous MOF Materials: The 40th Anniversary of International Zeolite Conference''. At the last IZC, MOFs were also classified into a new class of zeolitic materials.

approximately 15 Å in diameter. The hexagonal-shaped particle obviously corresponds to a [111] oriented cubic crystal, viewed along the three fold axis of the octahedron. HRTEM image simulations based on the structure model deduced from X-ray diffraction with the *Fd-3m* symmetry have been performed for different defocus and thickness values and confirm the interpretation that the bright dots do correspond to the tunnels. The simulation was in good agreement with the experimental image.

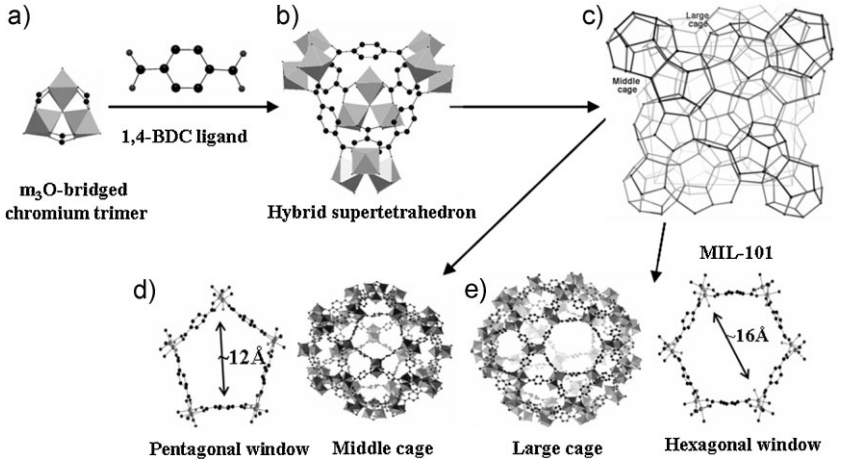

Figure 2. Basic building units and crystal structure of MIL-101.[51,52] a) Original building block with a trimer of chromium octahedral chelated by two carboxylic functions of organic ligand, b) hybrid superterahedron formed by using terephthalic acid, which occupies the edges of superterahedron, and c) a polyhedral representation of the 3D organization in the zeotype architecture of MIL-101 comprising two cages, which are present in a 2:1 ratio of middle and large cages: d) middle cages (20 ST, an internal diameter of ≈29 Å) with only pentagonal windows (free aperture ≈12 Å) and e) large cages (28 ST, internal diameter: 34 Å) with 12 pentagonal and 4 hexagonal windows (free aperture ≈14.5 Å × 16 Å).

3. Synthesis and Purification

Most syntheses of MOFs are generally performed by solvothermal or hydrothermal process via a co-operative ionic interaction between organic linkers containing di- and poly-carboxylate anions and inorganic cations including almost all di-, tri- and tetravalent elements, which form the skeleton of crystal frameworks together with solvent as a template.[14] As an alternative, the electrochemical synthesis was first introduced by a German company, BASF,[60] showing a novel route for a kilogram-scale production of MOFs. Recently, Chang and co-workers established a microwave route of MOFs,[61,62] which was already utilized for the synthesis of porous materials[63,64] as well as condensed solids.[65] In addition to the above-mentioned methods, ionothermal synthesis[66] with ionic liquids as both a solvent and ligand and high-throughput synthesis by combinatorial approach have also been studied.[67,68]

3.1. Hydrothermal Synthesis

During the syntheses of MOFs, the co-ordination of the metallic species, the nuclearity, and the dimensionality of the inorganic subnetwork are known to strongly depend on the temperature of reaction.[69–71] In the hydrothermal synthesis of MIL-101, synthesis temperature also influences the crystallization and condensation rates of inorganic chromium clusters. In general, the crystalline MIL-101 phase is favorably formed between 200 and 220 °C at pH < 2, indicating the relatively narrow temperature range for the synthesis. Synthesis time and concentration of solutes in the precursor solution are also important for the formation of MIL-101. For example, the product yield of MIL-101 increases up to 16 h at 210 °C in a typical condition but the new-phase MIL-53 then appears after 16 h. As concentrations of a chromium salt and terephthalic acid in the solution increase, the crystallinity of MIL-53 increases while that of MIL-101 decreases. The dependence of synthesis time and concentration of the solutes on the formation of both MIL-101 and MIL-53 can be ascribed to the slower nucleation of the MIL-53 phase than MIL-101 and thereby the longer induction period.

Loiseau and Ferey suggested that fluorine can act as a mineralizing agent to increase the crystallinity of microporous materials and favors the formation of highly crystalline phases in MOFs.[72] In the synthesis of zeolite beta, the fluoride

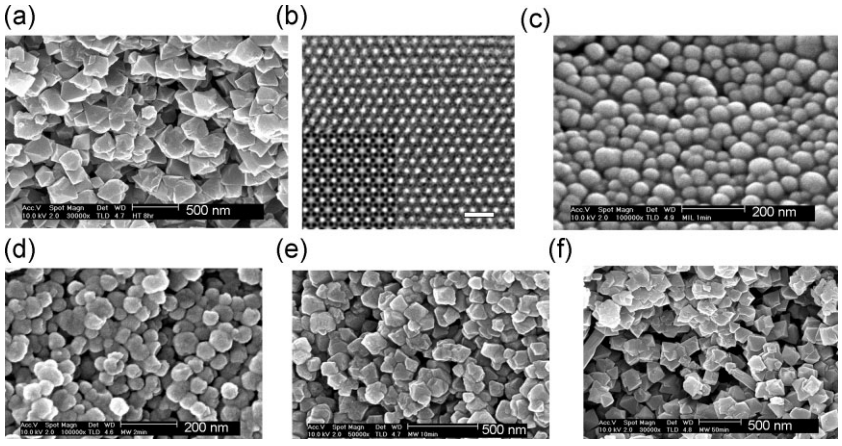

Figure 3. SEM and TEM images of MIL-101 prepared by hydrothermal and microwave methods: a) SEM and b) TEM images of MIL-101 prepared by hydrothermal method at 220 °C for 8 h;[59] SEM images of MIL-101 prepared with microwave method at 210 °C for various crystallization times:[61] c) 1 min, d) 2 min, e) 10 min, and f) 40 min.

anions appear to yield effective nuclei formation because it is assumed that the effect of fluoride mineralization leads to weakening of H-bonding for hydrated aluminosilicate precursors.[73] In the synthesis of chromium carboxylates, for example, MIL-100, fluorine has been considered as a mineralizing agent to increase the crystallinity and to promote the crystal growth of the final product. Actually, fluorine is involved in the terminal bond of the trimeric chromium species and partly substitutes the terminal water molecules attached to chromium in MIL-100.[72] Likewise, the effect of fluoride anions in the synthesis of MIL-101 under acidic conditions is believed to be similar to that of MIL-100. As the molar ratio of Cr/HF concentration in the precursor solution increases, the BET surface areas of as-synthesized MIL-101 increases from 2800 $m^2 g^{-1}$ to 3630 $m^2 g^{-1}$ (Fig. 4). It is not clear yet but it seems that the use of fluorine provides a strong interaction with chromium octahedral motif and the effective nuclei formation of MIL-101 during the hydrothermal reaction. However, further work is needed to fully understand the precise role of fluorine in the synthesis of MIL-101.

3.2. Microwave-Assisted Synthesis

The synthesis of MOFs, mainly carried out using hydrothermal or solvothermal methods, requires several days for their crystallization. Considering this drawback, synthesis is under microwave irradiation can provide an alternative because of its potential advantages including phase selectivity, narrow particle size distribution, facile morphology control, and efficient evaluation of process parameters besides fast crystallization.[74–77] However, this technique has recently been applied to the synthesis of porous MOFs[61,62,78–80] since the first report on microwave synthesis of MIL-100.[79]

For the porous chromium terephthalate, the microwave method provides the faster synthesis compared with the conventional way that needs 10 h at 220 °C.[61] Despite a slightly lower crystallization temperature (210 °C), the acceleration effect for the crystallization is very noticeable under microwave irradiation. The MIL-101 crystals obtained by the microwave method have very small dimensions with nanometer size especially for short crystallization times, as compared with those synthesized by the conventional hydrothermal method, as shown in the SEM images (Fig. 3c–f). The cubic symmetry of the MIL-101 is also reflected in the shape of the crystals synthesized by the microwave method (for a longer crystallization time of 40 min) as shown in the sample from the conventional hydrothermal method. Their dimensions increase with increasing crystallization time. In particular, the crystal sizes of MIL-101 obtained by microwave method range from 40 nm to 90 nm in the short synthesis time of a few minutes. There has also been very little effort toward making MOF nanoparticle,[61,81] although these could exhibit unique properties, as has been found for certain inorganic nanoparticles.[82] However, the above-mentioned result indicates that the microwave technique induces nanoparticles

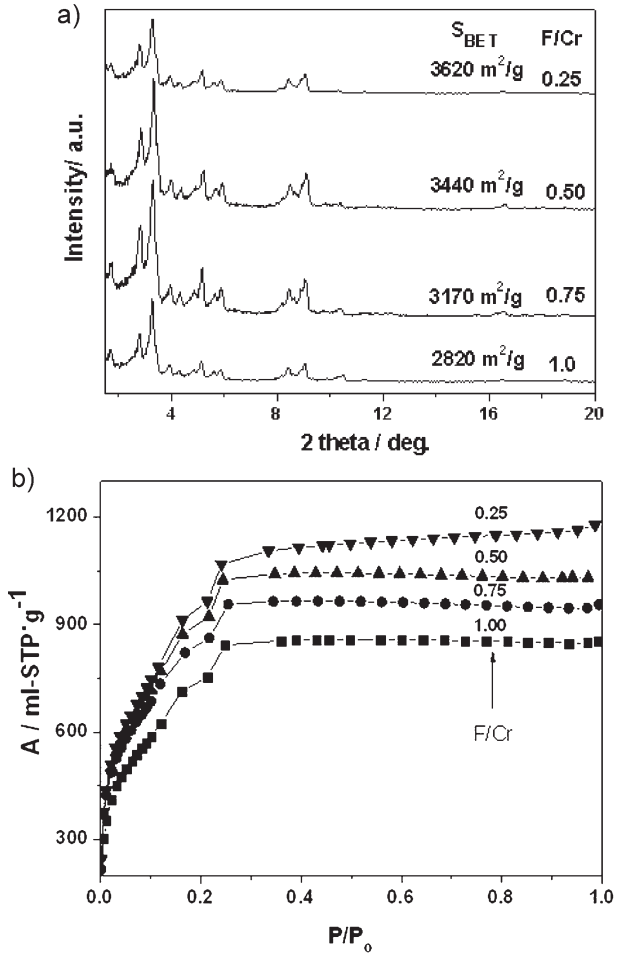

Figure 4. Effect of fluoride anion in the hydrothermal synthesis of MIL-101: a) XRD patterns and b) N_2 adsorption isotherms at -196 °C of MIL-101 prepared according to the different fluorine content at 210 °C for 8 h.

of MIL-101 as well as providing an easy control of crystal size. Therefore, the microwave method can offer a good opportunity for getting MOF nanoparticles.

Although the formation of porous hybrid materials under microwave irradiation is not well established yet, the faster synthesis of cubic chromium terephthalate appears to be accomplished through the fast dissolution of the precursor such as terephthalic acid or acceleration of the condensation of the metal–oxygen networks under microwave irradiation.[61] Considering the limited solubility of terephthalic acid in acidic conditions, it is necessary to quickly dissolve the acid for the nucleation and faster synthesis of the title compound. Microwave irradiation is believed to give rise to the fast dissolution of less-soluble precursor through selective heating of microwave-active species, leading to reduction of an induction period. For inorganic–organic hybrid compounds, it is known that carboxylate anions are multidentate ligands and the organic moiety acts as a template during the condensation of the metal–oxygen networks when synthesized under hydrothermal conditions.[14,18,83] Accordingly, the condensation step can be greatly accelerated by hot spots and superheating effect with microwaves,[64,84] resulting in the shortening of the overall synthesis time.

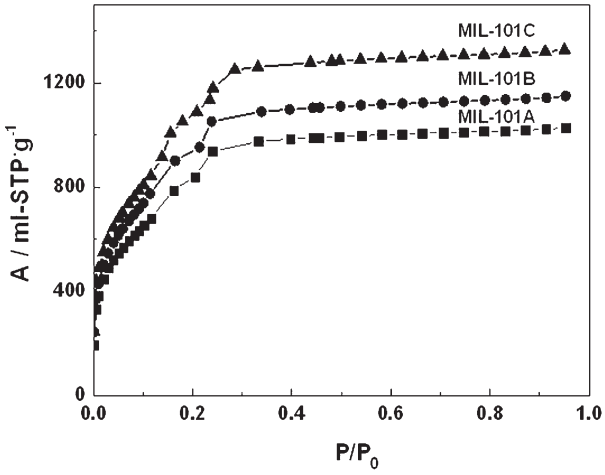

Figure 5. N_2 adsorption isotherms of MIL-101 at -196 °C according to purification steps: a) MIL-101A obtained after double filtration, b) MIL-101B obtained after solvent treatments with hot water/ethanol for MIL-101A, and c) MIL-101C obtained after aqueous NH_4F solution treatment for MIL-101B.

3.3. Purification of the As-Synthesized Product

Pure crystalline materials with high porosity and surface area are critically essential in terms of chemical and physical properties and of applications such as separation and catalysis.[85–87] However, substantial variations in surface area in MOFs, for instance, MOF-5 and $Cu_3(BTC)_2$, prepared according to different procedures have been reported.[88,89] Several possible reasons for the variations in the reported results include phase purity, crystal defects, and the presence of guest molecules (contaminants) in the samples prepared by different methods. Lillerud and co-workers pointed out that in MOFs, especially MOF-5 crystals showing the almost same XRD patterns there exists a big difference in surface area from 700 to 3400 $m^2\ g^{-1}$ according to the synthetic procedure because of $Zn(OH)_2$ species in the pores and of structural difference.[90] For $Cu_3(BTC)_2$, there have been continuous efforts to improve the synthesis and activation procedures.[91,92] It has been shown that the activation of this MOF material is particularly important for obtaining materials with high specific-surface areas and pore volumes.[92] Since the discovery of large-pore MIL-101, several groups have tried to synthesize MIL-101 for sorption applications.[93–97] However, it was hard to obtain crystalline MIL-101 with a high BET surface of more than 3200 $m^2\ g^{-1}$[52,53,98] because of the presence of organic or inorganic impurities in the pores as well as outside pores. As mentioned previously,[53] a significant amount of non-reacted terephthalic acid is present both outside and within the pores of MIL-101, leading to a decrease of its surface area and pore volume.

We have recently developed an effective purification method to produce MIL-101 with high BET surface. This method comprises three-step processes such as double filtration using two different filters, solvent treatments using hot ethanol and water, and fluoride–anion exchange using aqueous NH_4F solutions (see Experimental). In the purification with treatment of aqueous NH_4F solution, co-ordinated terephthalate anions exchanged with fluoride anions might be easily removed from the pores through the formation of ammonium terephthalate that is soluble in water. To confirm the effect of each purification step, the BET surface areas and pore volumes of MIL-101 according to the purification step were measured by N_2 adsorption experiments performed at −196 °C. As illustrated in Figure 5 and Table 1, the two-step treatments with hot ethanol/water and aqueous NH_4F solutions are quite effective in removing the residual terephthalic acid in the pores. After these whole treatments, the BET surface area of the dehydrated MIL-101 increases from 2800 $m^2\ g^{-1}$ to 4230 $m^2\ g^{-1}$ (Table 1). This result is evidence that the residual terephthalic acid species in the pores are largely removed by further solution treatments. Considering the similar effect using alkaline fluoride solutions, fluoride anion is believed to be essential in the removal of some terephthalate anions co-ordinated to CUS Cr(III) of MIL-101B. It is assumed that these treatments would be also effective in the removal of inorganic

Table 1. Texture properties of MIL-101 according to purification steps and comparison of their properties with those reported in the literature.

Samples	S_{BET} [$m^2\ g^{-1}$]	V_{pore} [$mL\ g^{-1}$]	Purification	Ref.
MIL-101A	2800	1.37	DF[a]	This work
MIL-101B	3780	1.74	DF and hot H_2O/EtOH	This work
MIL-101C	4230	2.15	DF, hot H_2O/EtOH, and NH_4F	This work
MIL-101	2931	1.45	DF1[b] and EtOH	[93]
MIL-101	2220	1.13	Hot DMF/EtOH	[94]
MIL-101	2693	1.30	OF[c] and H_2O	[95]
MIL-101	2578	1.25	DMF	[96]
MIL-101	3200	2.1	DMF	[97]

[a] DF: Double filtration with glass and paper filters (no 2 and 5). [b] DF1: Double filtration with glass filters (no. 2 and 1) and hot-water treatment. [c] OF: One-time filtration with glass filter (no. 1).

species such as chromium hydroxide trapped in the pores, as it was previously reported that metal hydroxides could be present in the pores of MOF-5.[85]

4. Physicochemical and Sorption Properties

4.1. Thermal Behaviour and Hydrothermal Stability

Thermal behaviour of MIL-101 was investigated using thermogravimetric analysis (TGA) in air to check the thermal stability. The TGA profile reveals that MIL-101 is stable up to 275 °C. We observed two steps of weight loss: the first step relates to guest water molecules in the range of 25–200 °C and the second one is responsible for the departure of OH/F groups and the framework decomposition of the organic moieties between 275 and 400 °C.

In spite of versatile advantages of porous MOFs including tailor-made pore structures and modulable porosity by change of organic ligands and metal ions, they have lower hydrothermal and chemical stabilities than inorganic porous materials or metal oxides due to the presence of organic backbones in the framework of MOFs. Moreover, when they are exposed to humid air some MOFs can easily collapse to amorphous phases as a result of easier hydrolysis of metal ions or metal clusters than that in inorganic moieties of inorganic zeolite materials.[89,99] In this respect, hydrothermal and chemical stabilities of MIL-101 are essentially important for further applications.

MIL-101 is stable over months under air atmosphere and when treated with various organic solvents at elevated temperature. Moreover, it is obviously stable even after exposure to boiling water at 100 °C for a week as illustrated in Figure 6. In contrast, even though highly cited MOFs, MOF-177 and MOF-5, have relatively high thermal and chemical stabilities, they are known to be unstable and easily decompose in the presence of moisture.[100,101] Therefore, the high hydrothermal stability, together with its high adsorption capacities, makes MIL-101 an attractive candidate for potential applications.

4.2. Outstanding Sorption Properties

The chromium(III) carboxylate MIL-101 has outstanding sorption properties for several gases, organic vapors, and even organic and inorganic compounds. Figure 7a shows the adsorption isotherms of N_2, O_2, and Ar on purified MIL-101 (MIL-101C) at −196 °C (N_2 and O_2) and −186 °C (Ar) after evacuation at 150 °C for 12 h. MIL-101 has higher adsorption uptakes of O_2 and Ar than that of N_2. The N_2 adsorption isotherm on the dehydrated MIL-101, and fitting the BET equation between $P/P_0 = 0.05$ and 0.2 to the resulting N_2 isotherm gives an estimated surface area of $S_{BET} = 4230\ m^2\ g^{-1}$. The total pore volume of MIL-101 is estimated to be $2.15\ cm^3\ g^{-1}$ by a single-point adsorption method. The isotherm has secondary uptakes at about $P/P_0 = 0.1$ and $P/P_0 = 0.2$, indicating the presence of the two nanoporous windows. The pore size distribution profile of MIL-101 calculated by BJH equation points out two monodisperse pores at about 15.0 Å and 19.3 Å, which are moderately higher than those estimated from crystal structure (≈12 Å and 16 Å × 14.5 Å).

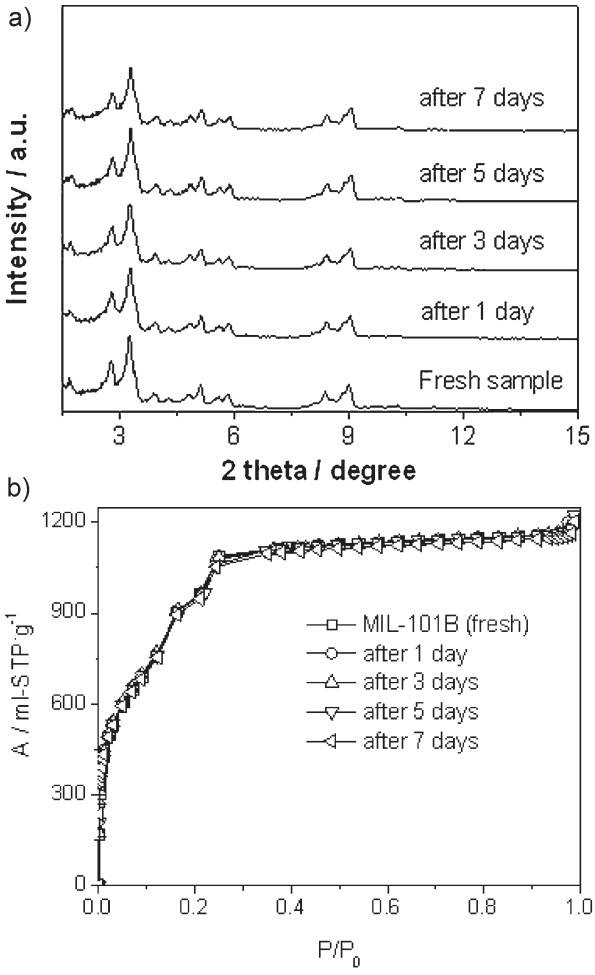

Figure 6. Hydrothermal stability of MIL-101B after exposure to boiling water at 100 °C for 7 days. a) XRD patterns and b) N_2 adsorption isotherms.

Carbon dioxide (56%) and methane (18%) are the two main greenhouse gases emitted today and methane is also an alternative fuel. Therefore, these gases are strategic in connection with global warming and energy problems.[102] In particular, MOFs present a valuable alternative for the removal of carbon dioxide and methane storage. High-pressure sorption studies on CO_2 and CH_4 have revealed that the large-pore chromium terephthalate MIL-101 adsorbs very large amounts of CH_4 and CO_2 at relatively high pressures (<50 atm) at 30 °C.[98] For carbon dioxide adsorption, no saturation is observed up to 50 atm (Fig. 7b). The carbon dioxide isotherms strongly depend on the activation method of MIL-101. The capacity at 50 atm and 30 °C increases from 28 mmol g^{-1} for MIL-101A and 34 mmol g^{-1} for MIL-101B up to a record value of 40 mmol g^{-1} in the case of MIL-101C. This leads to an unprecedented volumetric adsorption capacity of CO_2 per volume of adsorbent: 390 v/v for MIL-101C at 50 atm, well above the previous record (320 v/v for MOF-177 at 40 atm[103]). This makes these solids attractive candidates for high-pressure applications. The heat of adsorption of CO_2 at low coverage (−44 kJ mol^{-1}) is higher than those reported for MOFs[104] and on the same order of magnitude of zeolites.[105]

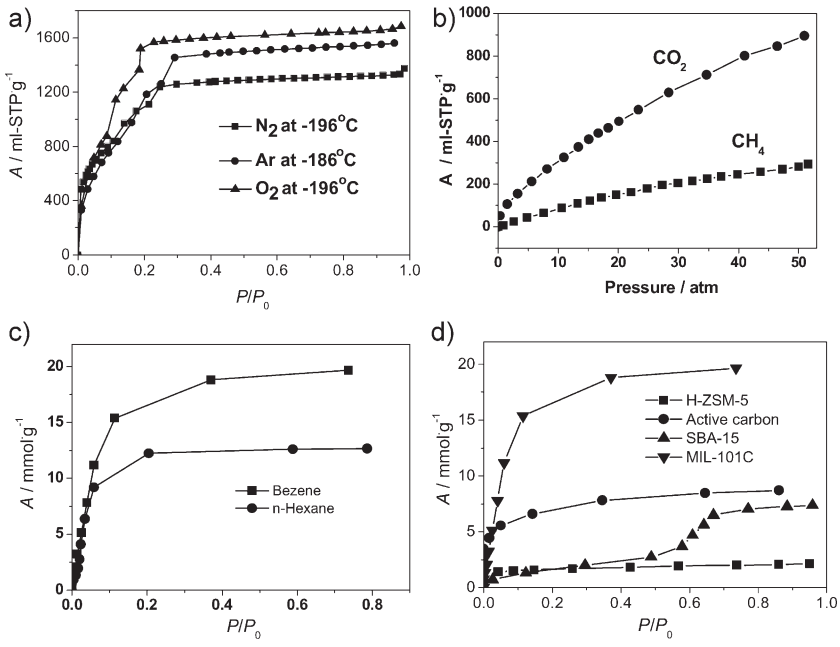

Figure 7. Sorption isotherms of light gases, benzene, and n-hexane of MIL-101C: a) sorption isotherms of N_2, O_2 and Ar at -196 °C (N_2 and O_2) or −186 °C (Ar), b) high-pressure sorption uptakes [98] of CO_2 and CH_4 at 30 °C, c) vapor-phase sorption uptakes of benzene and n-hexane at 32 °C, and d) sorption uptakes of benzene [61] on purified MIL-101 (MIL-101C) compared to commercial active carbon, H-ZSM-5, and mesoporous silica SBA-15.

The value is due to the co-ordination of the CO_2 molecules directly on the unsaturated chromium sites. However, the regeneration of MIL-101 during the CO_2 adsorption/desorption cycles is possible under mild conditions, unlike zeolites or mesoporous silicas.[106] Unlike CO_2, methane adsorption does not exhibit large differences in the MIL-101 samples obtained via the different purification steps.[98] According to our recent report, the methane uptake by MIL-101 (13.6 mmol g^{-1} at 60 atm) was higher than by MIL-100 (9.5 mmol g^{-1}).[98] In terms of volume, the capacity (135 cm^3_{STP} cm^{-3} at 60 atm) was slightly below that obtained with MIL-100 (150 cm^3_{STP} cm^{-3}). Saturation was not reached even at 80 atm. Furthermore, the enthalpies of adsorption of methane (−18 kJ mol^{-1}) were comparable to that of MIL-100 (−19 kJ mol^{-1}) at zero coverage, reflecting the moderate CH_4–host interaction.

Surprisingly, MIL-101 has also very high uptakes of organic vapors such as benzene and n-hexane. From vapour-phase sorption experiments, the equilibrium sorption capacity of n-hexane at 30 °C is 12.6 mmol g^{-1} at $P/P_0 > 0.7$ (Fig. 7c). Moreover, the sorption uptake of benzene is estimated to be 19.5 mmol g^{-1} at $P/P_0 > 0.7$, which is extremely large compared with the results adsorbed on various porous materials such as a mesoporous silica SBA-15 ($S_{BET} = 805\ m^2\ g^{-1}$), HZSM-5 zeolite (Zeolyst PQ, $S_{BET} = 550\ m^2\ g^{-1}$, $V_{pore} = 0.2\ cm^3\ g^{-1}$) and a commercial active carbon (Darco, $S_{BET} = 1600\ m^2\ g^{-1}$, $V_{pore} = 2.0\ cm^3\ g^{-1}$). The measured sorption capacities are 3.0, 1.9, and 8.0 mmol g^{-1} for SBA-15, ZSM-5, and the active carbon, respectively at $P/P_0 > 0.7$ (Fig. 7d). In spite of the smaller molecular size of the cylindrical n-hexane molecule (4.2 Å) compared to that of the spherical benzene molecule (5.85 Å), the higher equilibrium uptake of benzene than n-hexane indicates higher packing efficiency as well as π-interaction of benzene with sorption centers in the framework.[107]

The sorption experiments of benzene on MIL-101 that was prepared by the microwave method have also been accomplished in the liquid phase.[61] The sorption capacities on MIL-101 ($S_{BET} = 3900\ m^2\ g^{-1}$, $V_{pore} = 2.3\ cm^3\ g^{-1}$) and the commercial active carbon (Darco, $S_{BET} = 1600\ m^2\ g^{-1}$, $V_{pore} = 2.0\ cm^3\ g^{-1}$) were compared in aqueous solution containing 1000 ppm of benzene at 25 °C. Similar to the vapour-phase results, the MIL-101 (10.8 mmol g^{-1}) adsorbs a much higher quantity of benzene than the commercial active carbon (6.5 mmol g^{-1}). Additionally, the sorption rate of benzene is also high on MIL-101 compared with active carbon. The high and fast uptake of benzene in aqueous solution containing only 1000 ppm benzene indicates the high affinity of MIL-101 to benzene sorption taking into consideration the fact that the active carbon is hydrophobic and has a similar pore volume to MIL-101. The fast sorption behaviours show that hydrocarbons such as benzene can be readily adsorbed at low pressure, suggesting the potential application of MIL-101 in the sorptive removal of volatile organic compounds (VOCs).

5. Selective Functionalization of Unsaturated Sites

5.1. Coordinatively Unsaturated Chromium(III) Sites

The existence of co-ordinatively unsaturated metal sites (CUS) is very beneficial in porous materials.[53,108–112] For example, MOFs with CUS, due to the regular arrangement and well-understood surrounding environments of metal centers in the pore channels, could be used to induce regioselectivity and shape or size selectivity towards guest molecules or reaction intermediates.[113,114] Unlike inorganic zeolites and mesoporous materials, MOFs are able to generate CUS in the pore channels during the formation of open frameworks through the 3D covalent connection of inorganic and organic parts. The presence of CUS in MOFs would be beneficial for further functionalization, leading to applications in catalysis and sorption.

Indeed, trimeric chromium(III) octahedral clusters of MIL-101 possess terminal water molecules, removable from the framework after vacuum treatment at 150 °C for 12 h, thus providing the CUS as Lewis acid sites in the structure usable for the surface functionalization (Fig. 8a). After purification of the as-synthesized solid, which contained occluded terephthalic acid[29,98] and activation (150 °C, 12 h), in situ IR analysis of the dehydrated MIL-101 upon CO adsorption reveals 1.0 mmol g^{-1} of CUS

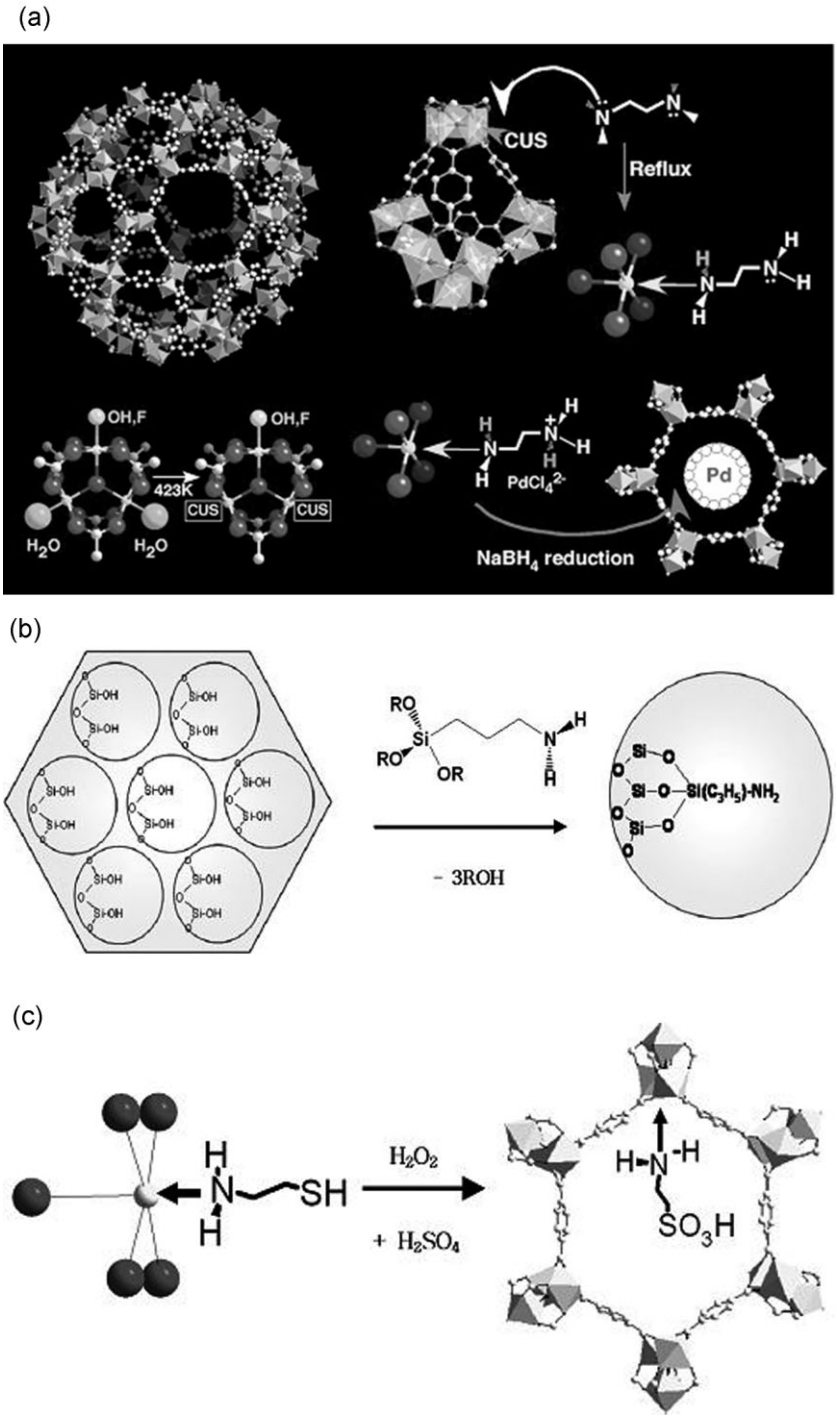

Figure 8. Schematic views of surface functionalization of MIL-101 and mesoporous silica: a) site-selective functionalization of MIL-101 through selective grafting of chelating ligands onto coordinatively unsaturated chromium sites,[53] b) functionalization of mesoporous silica wall by alcoholysis of surface hydroxyl group and ethoxy group of aminopropyltriethoxy silane, [53] and c) sulfonic acid-functionalization of MIL-101 via thiol incorporation with cysteamine and post-oxidation with H_2O_2 and H_2SO_4.

Cr(III) in the framework, indicating the presence of residual terephthalic acid co-ordinated to CUS.

5.2. Surface Functionalization with Amine Grafting

The search for a new modification method to functionalize pore channel and cavities in MOFs is crucial for extending the application of these new hybrid materials. Moreover, introduction of functionality into the channel of MOF materials may spread its diverse importance in catalysis, encapsulation of metal nanoparticles, and functionalized thin films. Regarding the functionalization of MOFs, there have been so far three approaches: a) pre-modification of organic linkers with functionalized ligands,[115,116] b) post-covalent modification with functionalization of organic ligands or linker sites,[117,118] and c) post-grafting of CUS with chelating agents or electron-rich molecules.[53] For example, Chui et al. reported that the channel linings of a porous metal co-ordination polymer can be chemically functionalized, for example, the aqua ligands can be replaced by pyridine.[110] Post-synthetic modification of a ligand in IRMOF-3 was covalently functionalized by acetylation.[117] It has been also reported that the cavities of MOFs can be easily modified by chemical modification without change of the original crystal structure.[118] Importantly, Kitagawa and co-workers proposed two smart strategies on this point: immobilization of CUS[115] and introduction of functional organic sites[116] to decorate channel surfaces of coordination polymers, but these strategies include only the functionalization of ligand and incorporation of low-co-ordination metal centers in the primary synthesis. However, in spite of several reports on the utilization of CUS in MOFs, there has yet been no strategy for the direct utilization of CUS for the surface functionalization except our recent work.[53]

Amines with a functional group of alkoxysilane are often used as grafting reagents, particularly with mesoporous silicas for their applications in base-catalyzed reactions[119] and the immobilization and encapsulation of large molecules.[120,121] In fact, the amine-grafted mesoporous silicas have been widely investigated because of their versatile applications, but hydroxyl groups on the surface are needed to prepare these materials. The grafting pathway in mesoporous silica using 3-aminopropyltriethoxysilane (APS) is depicted in Figure 8b. However, a drawback in the use

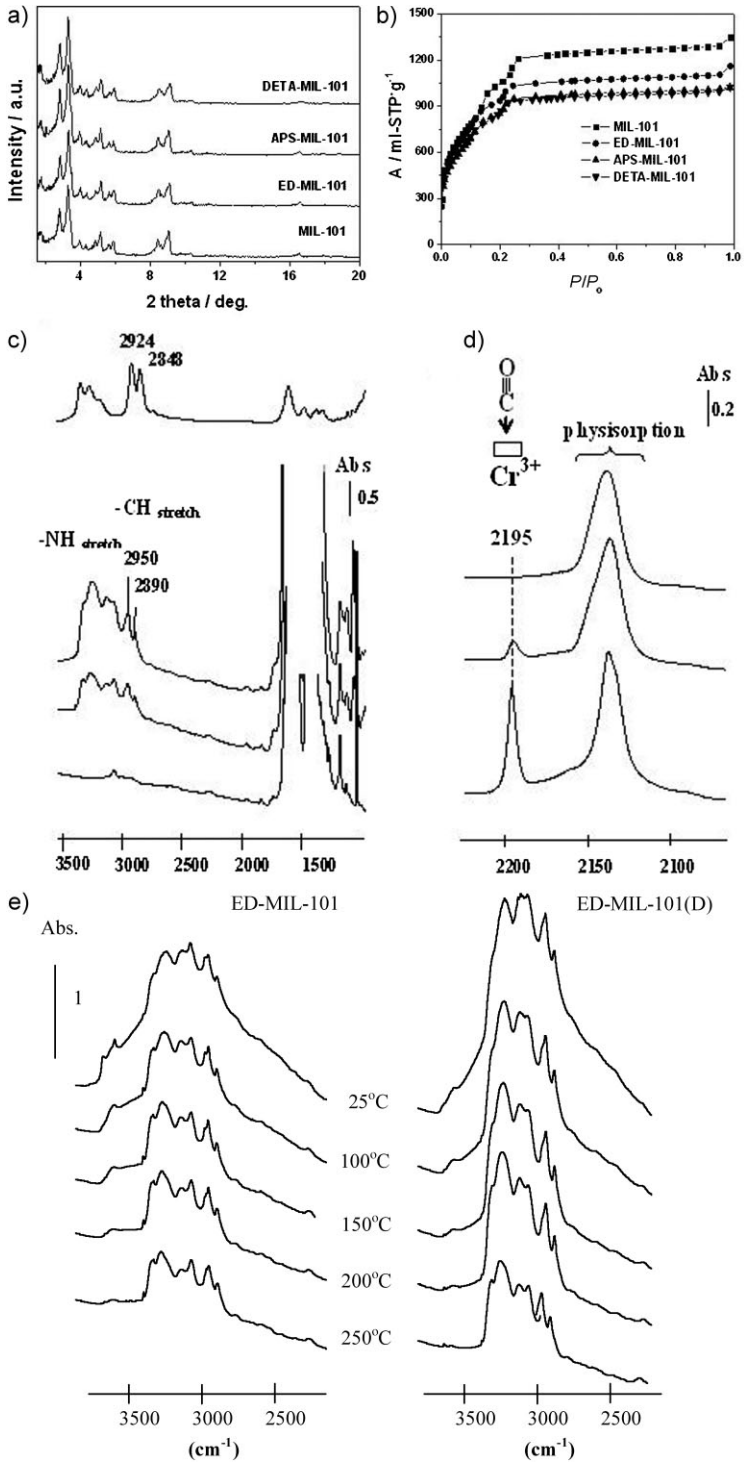

Figure 9. a) XRD patterns and b) N_2 adsorption isotherms of as-synthesized and amine-grafted MIL-101 at -196 °C after vacuum treatment −150 °C for 12 h;[53] IR spectra of the grafted MIL-101, CUS Cr(III) characterization, and thermal stability of grafted MIL-101:[53] c) IR spectra of MIL-101, ED-MIL-101 and ED-MIL-101(D) outgassed at −150 °C and of ED in liquid phase from bottom to top, and d) infrared spectra recorded at −173 °C of MIL-101, ED-MIL-101 and ED-MIL-101(D) outgassed at 200 °C after introduction of an equilibrium pressure (200 Pa) of CO from bottom to top, and e) thermal stability of grafted samples under vacuum, followed by FT-IR: IR spectra of ED-MIL-101 (left) and ED-MIL-101(D) (right) outgassed under vacuum (10^{-4} Pa) during 15 min at room temperature up to 250 °C.

of a popular grafting agent, APS for mesoporous silica is known to be hampered by the variety and complexity of surface amine species through the inter- and intramolecular H-bondings between an aminopropyl group of APS and surface hydroxyl groups of mesoporous silica.[122] In contrast, the direct utilization and functionalization of MOFs have been largely unexplored due to the lack of surface hydroxyl groups available in porous hybrids and their limited pore sizes, typically less than 10 Å.

For the selective functionalization of CUS, we chose first an effective grafting reagent with multifunctional chelating groups, ethylene diamine (ED). As illustrated in Figure 8a, if one amine group of ED is linked to CUS Cr(III) of MIL-101 by direct ligation, the other amine group can play the role of immobilized base catalyst.[123] Clearly, this concept does not apply to the surface functionalization of mesoporous silicas because of their lack of unsaturated surface sites in general (Fig. 8b).

To prove this concept, the synthesis of the ED-grafted MIL-101 (ED-MIL-101) by co-ordination of ED to the dehydrated MIL-101 framework was performed in toluene under reflux conditions.[53] Diethylene triamine (DETA) and APS can be also used for the surface functionalization. However, it is noted that APS has been sometimes problematic when it was used for the functionalization of MIL-101. Since two different functional groups, terminal amine and ethoxy groups in APS could be independently co-ordinated to CUS each other in the grafting, the resulting terminal amine groups in the APS-grafted MIL-101 was actually very sensitive to the grafting conditions. The almost unchanged X-ray diffraction patterns (XRDP) show that the ED grafting occurs with no apparent loss of crystallinity (Fig. 9a) with, however, some slight variation of the Bragg intensities. The resulting pore modification is visible on the N_2 adsorption isotherms of the amine-grafted MIL-101. Compared with the pristine MIL-101, they exhibit a significant decrease of the N_2 amount adsorbed at $P/P_0 > 0.01$ (Fig. 9b). The BET surface area decreases from 4230 m^2 g^{-1} to 3555 m^2 g^{-1} after grafting. The pore size distribution curves indicate that the amine grafting leads to a slight decrease of the pore sizes.[53] The grafted amine groups are assumed to be present mainly at the center of mesopore cages leading to a slight decrease of the pore sizes because terminal water molecules produce a CUS Cr(III) point at the center of the cages.

The IR spectra of the self-supported ED-MIL-101 wafer dehydrated at 150 °C for 12 h under vacuum confirm the grafting. Figure 9c shows the spectra of the bare MIL-101 compound compared with the two samples after ED grafting; the ν(NH) and ν(CH) stretching regions evidence the presence of ED, the spectrum of which is also reported in the liquid phase, for comparison. It is worth noting that the observed aliphatic C–H stretching vibrations (2800–3000 cm^{-1}) are upward shifted, as observed when the molecule is coordinated to a Lewis acid center,[124] therefore clearly demonstrating the selective ED grafting onto CUS Cr(III) in mesoporous cages. Furthermore, as shown on Figure 9d, the concentration of CUS Cr(III) detected by CO adsorption at low temperature undoubtedly decreases with increasing amount of coordinated ED. Infrared spectra recorded after outgassing of ED-MIL-101 with increasing temperatures confirm the stability of amine species at least up to 200 °C, as shown in Figure 9e.

The concept of amine grafting onto CUS can be extended to sulfonic acid grafting, which is useful for solid acid catalysis. In general, sulfonic acid-functionalized silicas are based on the covalent attachment of alkylsulfonic acid groups to the surface of mesoporous silicas through the functionalization with propane thiol groups by reaction of the surface silanols with 3-mercaptopropyltrimethoxysilane (MPTMS) as the key precursor.[125] For MIL-101, however, cysteamine ($NH_2CH_2CH_2SH$) was used as a grafting reagent to prepare the sulfonic acid-functionalized material. As illustrated in Figure 8c, the grafting procedure comprises two steps: thiol incorporation and post-oxidation. Thus, the grafting of cysteamine ($NH_2CH_2CH_2SH$) on the dehydrated MIL-101 was performed in an anhydrous ethanol solvent under reflux condition to form the thiol-grafted MIL-101 (SH-MIL-101). The subsequent oxidation of surface thiol was then carried out using diluted H_2O_2 at 45 °C, followed by acidification with 0.1 M H_2SO_4 at room temperature. Thus the obtained materials were further characterized by IR spectroscopy, showing signals at 1245 cm^{-1} and 661 cm^{-1}, corresponding to the symmetric stretching vibrations of S=O and S–O, respectively, for the sulfonic acid-grafted one. After grafting of –SH and $–SO_3H$ groups, the BET surface area decreases from 4230 m^2 g^{-1} to 3170 and 2200 m^2 g^{-1}, respectively. XRD patterns of sulfonic acid-functionalized SO_3H-MIL-101 shows no big difference compared to as-synthesized MIL-101, but intensity of the first peak in XRD is slightly changed, indicating the successful functionalization.

6. Encapsulation of Nano-objects

6.1. Metal Encapsulation

The concept of amine-grafting on CUS has led to a very important consequence, that is, the encapsulation of metals for which only few attempts have been made until now.[14,126–129] For example, Fischer and co-workers have performed the loading of metals such as Pd and Cu onto MOF host lattices by the adsorption of metal–organic CVD precursors.[126,127] Although the range of observed nanoparticle sizes is above the dimensions of the cage, the corresponding solids exhibited distinct catalytic properties. Paik Suh and co-workers have tried to generate in situ nanoparticles of Ag and Au within a flexible Ni-containing MOF through the reduction of noble metals by the Ni^{2+} of the cyclam complex.[128] The Ni-containing MOF network was intact, while the generated nanoparticles were not incorporated between the layers. Kaskel et al. proposed that the loading of MOFs with metal particles may be possible by the ''incipient wetness'' method, for example, to prepare Pd@MOF-5 with about 1 wt % Pd loading.[129] Fischer and co-workers recently demonstrated the well-defined inclusion compound $[Ru(cod)(cot)]_{3.5}$@MOF-5 was derived, and then hydrogenolysis to form Ru nanoparticles in a typical size range of 1.5–1.7 nm inside the cavities was performed, leading to a material denoted as Ru@MOF-5.[54] Despite previous efforts, inclusion of metallic nanoparticles in MOFs still remains a challenge.

We have succeeded in the encapsulation of noble metals[53] such as Pd, Pt, and Au over the amine-grafted MIL-101 according to the procedure depicted in Figure 8a. The encapsulation procedure comprises the neutralization of the surface amine groups with an aqueous HCl solution, ionic reactions of the positively charged surface ammonium groups with anionic noble metal salts, that is, $PdCl_4^{2-}$, $PtCl_6^{2-}$, and $AuCl_4^-$, by anionic exchange of chloride anions, and finally the gentle reduction of noble metals with excess $NaBH_4$ at low temperature. After the encapsulation of noble metals, there is no apparent loss of crystallinity in XRDP; no supplementary Bragg peaks appear but the intensities of those of MIL-101 change specifically to each metal, confirming their introduction in the pores (Fig. 10a). The BET surface area slightly decreases from 3250 m^2 g^{-1} to 2910 m^2 g^{-1} after Pd encapsulation (Fig. 10b) although in this case, ED-MIL-101 was made with different MIL-101C ($S_{BET} = 4090$ m^2 g^{-1}). TEM images of 1 wt% noble-metal-containing MIL-101 materials (0.93–0.96 wt% based on ICP analysis) also support the successful encapsulation with the detection of fine nanoparticles in the range of 2–4 nm (Fig. 10c), in agreement with the cage diameters, although some of nanoparticles remain outside the pores.

6.2. Encapsulation of Keggin Polyanions and Drugs

The large windows of MIL-101 easily allow the introduction of new species into the cages and possible enhanced reactions favored by confinement effects in the cages.[52] Moreover, once introduced nanometric species fill the pores and the fixed dimensions of the pores lead to monodisperse nanomaterials on the scale of 1 to 3 nm. The possibility of their introduction depends on the correlation between their size and the accessible dimensions of the windows of each cage. Large species may tend to occupy only the large cages (ca. 20 600 $Å^3$) while leaving space for other species with different properties in the medium cages (ca. 12 700 $Å^3$). In fact, MIL-101 allows the introduction of large molecular inorganic species[52] and drugs[38] within the mesoporous cages. For instance, MIL-101 incorporates the Keggin polyanion ($PW_{11}O_{40}^{7-}$).[52] Owing to the large dimension of this anion (ca. 13 Å), only the large cages can host it. From XRPD, TGA, specific surfaces and solid-state ^{31}P NMR measurements, it was proved that each cage can accept five Keggin ions, representing 50% of the volume of the cage.[52] Quantitative

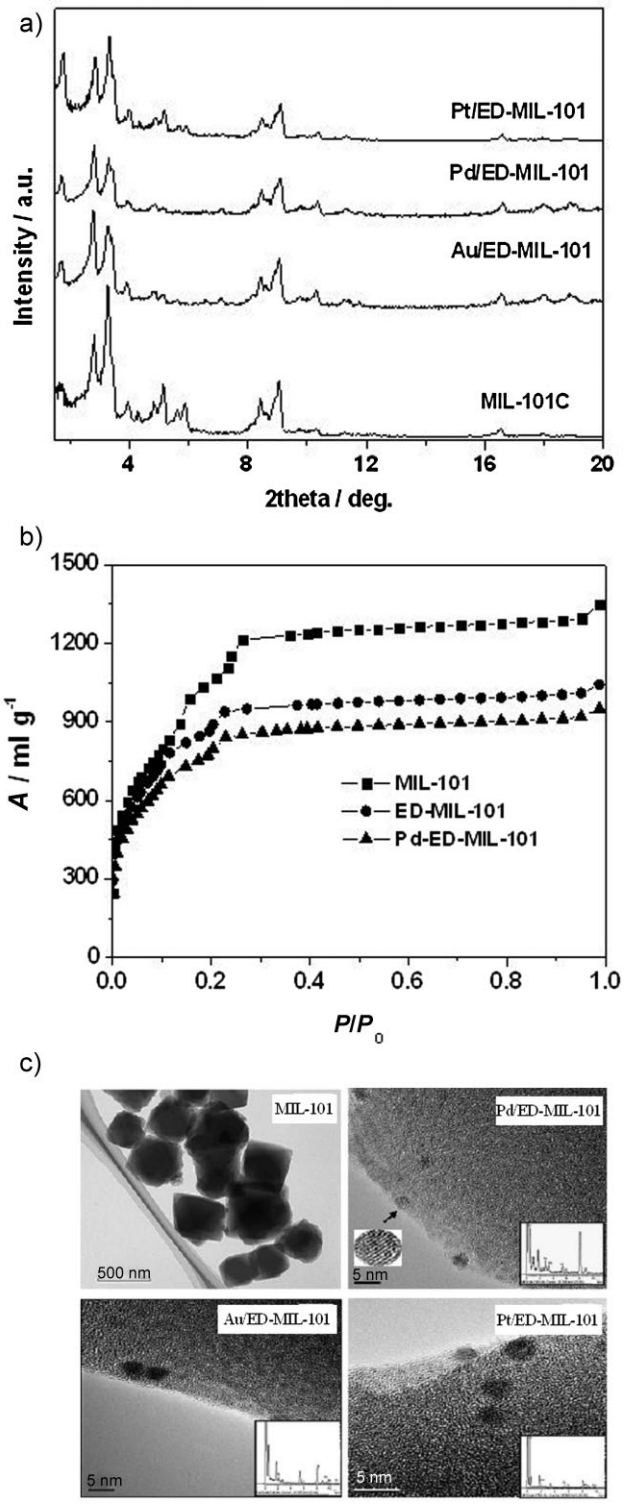

Figure 10. a) XRD patterns of as-synthesized and precious metal-encapsulated ED-MIL-101 with 1 wt% Pd, Pt or Au; b) N_2 isotherms of MIL-101, ED-MIL-101 and Pd-ED-MIL-101, respectively; c) TEM images[53] of as-synthesized MIL-101 and precious metal encapsulated ED-MIL-101.

analysis also gave an estimation of ~0.05 Keggin anions per chromium. Considering the size of the $K_7PW_{11}O_{40}$ ion, we assumed that the polyanions could diffuse into the largest cages only, which would allow about five highly charged Keggin moities per large cage (Keggin anions per cage, ~5.3). Because the volume of a $PW_{11}O_{40}^{7-}$ anion is nearly 2250 A^3, five Keggin ions represent ~10 100 A^3 in volume, which is lower than the ~20 600 A^3 volume of a large cage. The residual volume is probably occupied by cations and water molecules.

This successful incorporation of large amounts of Keggin anions strongly suggests that MIL-101 is an ideal candidate for the introduction of other nano-objects in a regular and monodisperse mode with specific physical properties or for drug delivery. Some of us recently demonstrated that the windows of MIL-101 allow the introduction of large molecular species, particularly drugs.[38] The analgesic Iboprofen was used as a probe for validation.[130] Considering the molecular size of Ibuprofen (6×10.3 Å), two mesoporous cages in MIL-101 are able to occlude ibuprofen molecules. Indeed, MIL-101 showed remarkable Ibuprofen uptake (1.4 g $g^{-1}$of dehydrated MIL -101) compared to what was known before.[38] This result indicated that each medium and large cage of MIL-101 hosts approximately 56 and 92 Ibuprofen molecules, which represent four times the capacities of MCM-41 toward Ibuprofen[130] according to the weight increase. Moreover, it is highlighted that it took 6 days to the complete drug release with MIL-101, which may be due to the high proportion of aromatic rings in MIL-101,[38] leading to an increase of the number of interactions between the Ibuprofen and the pore surface of MIL-101.

7. Catalytic Applications

Although catalysis is one of the most important applications of MOF materials, as in the case of microporous zeolites and mesoporous materials, only a handful of examples have been so far reported.[14,32,131] For catalytic applications using MOF materials, apparently five types of catalyst systems or active sites have been utilized:[14] a) homochiral MOFs, b) metal ions or ligands in MOFs, c) CUS in MOFs, d) metal complexes in supramolecular porous frameworks, and e) highly disperse metal or metal oxide nanoparticles loaded onto porous MOF host lattices. In this work, we showed catalytic applications by CUS Cr(III) species, surface-grafted amine species, and encapsulated palladium species in MIL-101.

The formed CUS can provide accessible sites for guest molecules, therefore playing a role as Lewis acid sites[132] or catalytically active sites.[37] Indeed, the presence of CUS Cr(III) center in MIL-101 has found to provide the oxidation ability of aryl sulfides to selectively produce the corresponding sulfoxides in the presence of hydrogen peroxide.[133] Oxidative competition reactions induced by the CUS Cr(III) center indicate that electron-releasing groups of aryl sulfides enhance the oxidation reactivity.

In line with a successful immobilization of a Keggin heteropolytungstate within the cages of MIL-101,[52] Maksimchuk et al. also reported that polyoxometalate (POM) such as Co- and Ti-monosubstituted Keggin-type heteropolyanions can be attached electrostatically to the surface of MIL-101 to produce the composite POM/MIL-101 materials.[97] These composite materials showed

Table 2. Texture properties of the amine-grafted MIL-101 and mesoporous silica SBA-15 and their catalytic properties in the Knoevenagel condensation with benzaldehyde and ethyl cyanoacetate.[53]

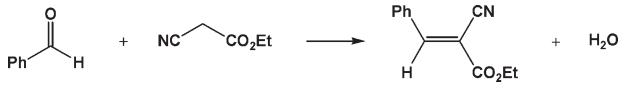

Catalysts[a]	S_{BET} [m^2 g^{-1}][b]	N-contents [mmol/g-catalysts][c]	Conv. [%]	Sel [%]	TOF [h^{-1}][h]
ED-MIL-101	3555	2.07 (1.04)[d]	97.7[e]	99.1[e]	328
ED-MIL-101(D)	3257	3.96 (1.98)[d]	97.7[f]	99.3[f]	214
ED-MIL-101(T)	3010	4.67 (2.34)[d]	97.3[f]	99.3[f]	189
DETA-MIL-101	3215	3.03 (2.02)[d]	97.7[e]	99.3[e]	190
APS-MIL-101	3306	1.14	96.3[e]	99.3[e]	168
APS-SBA-15	510	2.89	74.8[g]	93.5[g]	32

[a] Reaction was carried out with 10 mmol of benzaldehyde, 10 mmol of ethylcyanoacetate, and 20 mg of catalytst in 25 mL of cyclohexane at 353 K. [b] S_{BET}: BET surface areas obtained from N2 adsorption isotherms. [c] Determined by elemental and thermogravimetric analyses. [d] Number in each parenthesis denotes the content of free amine group(s) available for the reaction. [e] The reaction time was 19 h. [f] The reaction time was 7 h. [g] The reaction time was 16 h. [h] TOF (turnover frequency): Moles of product formed per mole of nitrogen of free amine group(s) in the grafted MIL-101 or the grafted SBA-15 per hour. The TOF values are calculated by the use of initial activity data taken at 20 min, which are linear to the reaction time.

fairly good catalytic activity and selectivity in the liquid-phase oxidation or epoxidation of alkenes including cyclohexene, α-pinene, and caryophyllene with O_2 or H_2O_2. It has been shown that these materials are stable to POM leaching, behave as true heterogeneous catalysts, and can be used repeatedly without sustaining a loss of activity and selectivity in oxidations.

The catalytic performances of dehydrated ED-MIL-101 in base catalysis were measured using the Knoevenagel condensation as a base-catalyzed model reaction[53] and were compared to those of the APS-grafted mesoporous silica SBA-15 (APS-SBA-15). Table 2 shows catalytic results of the condensation of benzaldehyde with ethyl cyanoacetate over various amine-grafted molecular sieves at 80 °C. Interestingly, for only a small amount of catalyst (20 mg or 0.8 mM), the catalytic activities of ED-MIL-101 are noticeably better than those of APS-SBA-15 even though the content of free amine groups in ED-MIL-101 (1.04 mmol/g) is significantly lower than that of APS-SBA-15 (2.89 mmol/g). For the condensation of benzaldehyde into *trans*-ethyl cyanocinnamate, the conversion for ED-MIL-101 is 97.1% with high selectivity (99.1%). By contrast, the APS-SBA-15 exhibits only 73.8% conversion with 93.5% selectivity. Moreover, in terms of turnover frequency (TOF), ED-MIL-101 shows a remarkably superior activity (11 times higher than that of APS-SBA-15). The higher activity of ED-MIL-101 might be mainly attributed both to the easily accessible amine functional groups and to its high surface area. As already mentioned in Section 5.2., the lower activity of APS-SBA-15 can be ascribed to the actual loss of catalytically active sites by the formation of H-bondings between functional groups.[122] The DETA- and APS-grafted MIL-101 (DETA-MIL-101 and APS-MIL-101) show also much higher activities than APS-SBA-15 (Fig. 11a, Table 2). At the end of each catalytic reaction such as the Knoevenagel condensation and Heck reaction, the catalyst was

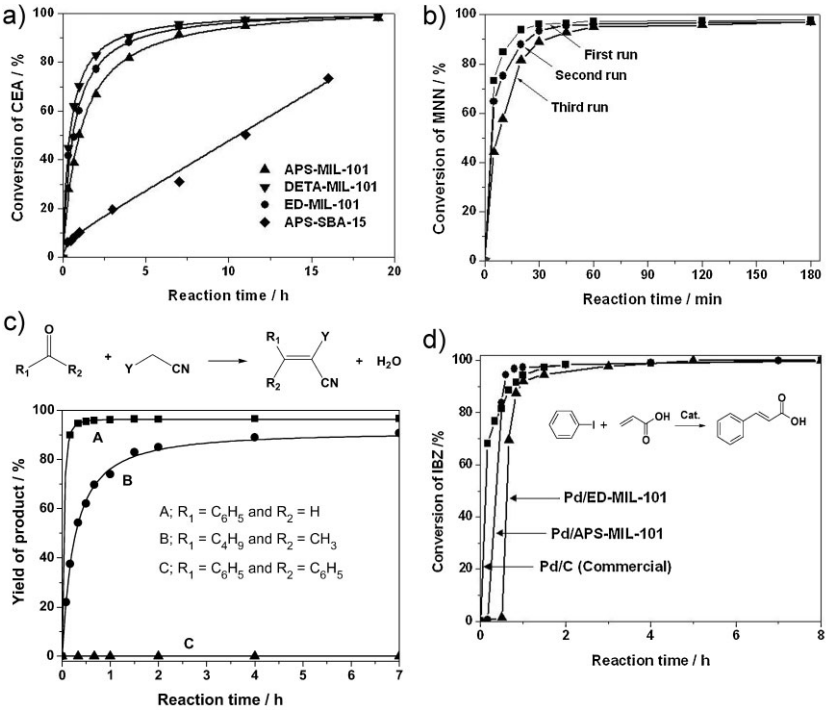

Figure 11. Catalytic activities of amine-grafted MIL-101 and Pd-loaded MIL-101:[53] a) catalytic activities of amine-grafted MIL-101 and APS-grafted SBA-15 in Knoevenagel condensation with benzaldehyde (BZA) and ethylcyanoacetate at 80 °C; b) the recyclability test of ED-MIL-101 in Knoevenagel condensation with benzaldehyde (BZA) and malononitrile (MNN) at 80 °C; c) product yields as a function of reaction time in the Knoevenagel condensation over ED-MIL-101 with various substrates at 80 °C. Reaction was carried out with 10 mmol of carbonyl compounds, 10 mmol of the selected nitrile compound, and 50 mg of catalyst in 25 mL of toluene at 80 °C; d) catalytic activities of palladium-loaded MIL-101 and commercial Pd/C as a function of reaction time in the Heck coupling reaction. Reaction was carried out with 10 mmol of iodobenzene (IBZ), 15 mmol of acrylic acid, 15 mmol of triethylamine and 50 mg of catalyst in 25 mL of N,N-dimethylacetamide as a solvent at 393 K.

Table 3. Catalytic activities of ED-MIL-101 in the Knoevenagel condensation depending on various reactant substrates. Reaction was carried out with 10 mmol of aldehyde compounds, 10 mmol of cyanate compounds, and 50 mg of catalyst in 25 mL of solvent at 80 °C.

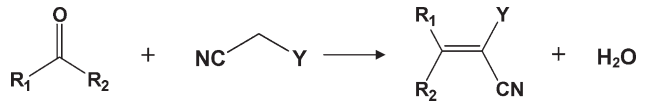

Entry	R_1	R_2	Y	Solvent	Time [h]	Yield [%]
1	C_2H_5O	CH_3	CN	Toluene	17	31.6
2	C_4H_9	CH_3	CN	Toluene	9	90.0
3	CH_3	H	CN	Toluene	1.5	93.6
4	C_6H_5	CH_3	CN	Toluene	17	51.4
5	C_6H_5	C_2H_5	CN	Toluene	17	24.7
6	C_6H_5	H	CN	Toluene	0.7	96.0
7	C_6H_5	C_6H_5	CN	Toluene	17	–
8	C_6H_5	H	$CO_2C_2H_5$	Toluene	5	97.7
9	C_6H_5	H	$CO_2C_2H_5$	Cyclohexane	5	98.7
10	CH_3	CH_3	$CO_2C_2H_5$	Toluene	9	48.1

isolated from the reaction solution, dried at 150 °C, and then reused in the second run of each reaction. The initial activity of the catalyst was also obtained in the second run, showing that the framework of the catalyst may remain intact during the catalytic cycles. The catalyst remained effective for up to 3 cycles for reactions (Fig. 11b). Further proof was obtained with a separation experiment. After removal of the catalyst by filtration, no further reactivity was exhibited in the filtrate. The catalyst used in the second run was also analyzed by XRD, but no significant change was observed. Therefore, the recyclability test[53] of ED-MIL-101 clearly supports that it is easily isolated from the reaction suspension by filtration and can be reused without significant loss of activity in the third run.

ED-MIL-101 exhibits high catalytic activities for various substrates in the Knoevenagel condensation (Fig. 11c, Table 3). Dimethyl ketone, benzaldehyde, and methylbutyl ketone are found to be collected as good substrates producing more than 90% conversion to adducts in the condensation with ethylcyanoacetate or malonitrile. Remarkably, ED-MIL-101 reveals the size dependence on catalytic activities due to the change of the substituent groups of carbonyl compounds in the Knoevenagel condensation. For example, with benzophenone, the condensation reaction with malonitrile (Entry No. 7) is hard to realize because the formation of the quite large product, diphenyl methylene malononitrile might be occluded in the pores, indicating the transition state or product shape-selectivity already known in microporous zeolites.[134] The size-selective reactivity in ED-MIL-101 points out that the reaction essentially takes place in the amine-grafted pores taking into consideration the guest-selective properties of a 3D porous coordination polymer with amide groups in the base-catalyzed Knoevenagel condensation.[116] This result also led to tune the pore size of MIL-101 by the type and shape of grafting agents leading to the pore modification.

Besides the base-catalyzed reaction, we have tested catalytic activity of SO_3H-functionalized MIL-101 in acid catalysis (see Supporting Information Fig. S1). When the catalytic performance was preliminarily examined in the esterification of acetic acid with ethanol at 100 °C, the SO_3H-functionalized MIL-101 with S/Cr = 0.67 (molar ratio) exhibited an increased activity (70.1% conversion of acetic acid at 30 h) as compared with the activity of MIL-101 (24.7% conversion at 30 h).

Pd-loaded APS-MIL-101 (Pd: 0.93 wt%) and ED-MIL-101 (Pd: 0.95 wt%) exhibit high activities (Fig. 11d) during the Heck reaction at 120 °C, which is the most powerful method to couple alkenes with organic moieties.[135] When the coupling reaction of acrylic acid with iodobenzene was concerned, their activities were comparable with that of a commercial Pd/C catalyst (1.09 wt% Pd) after a certain induction period (0.5–1 h), probably due to the slow diffusion of reactants to reach accessible metal sites in the pores. The recyclability test of Pd-loaded MIL-101 confirmed that the reaction takes place mainly in a heterogeneous manner.

8. Conclusions

A great deal has been investigated over recent years about how to develop smart MOFs with hierarchical pore structures and unprecedented properties that are not observed in conventional porous materials, and how to functionalize them for potential applications. Chromium terephthalate MIL-101 can be a candidate to fulfil these requirements because it has a unique and hierarchical pore structure with multiple pores between 8–35 Å as well as unsaturated chromium sites besides outstanding sorption properties due to its huge surface area and pore volume. The highly porous chromium terephthalate has been hydrothermally synthesized from chromium(III) salts and terephthalic acid in the presence of HF at 200–220 °C. The microwave method provided a very short crystallization time for MIL-101 within 5–40 min as well as an easy way of making the nanoparticles. We have also developed an effective purification method to produce high-surface-area MIL-101 with more than 4000 m^2/g. This method comprised three-step processes such as double filtration, solvent treatments, and fluoride anion exchange. Thus purified MIL-101 exhibited outstanding sorption properties for several gases, organic vapors, and even organic and inorganic compounds. This solid has potential as a nanomold for monodisperse nanomaterials, as illustrated here, within the cages. The co-ordinatively unsaturated sites in MIL-101 have been selectively functionalized, in a way differing from the functionalization of mesoporous silica and porous hybrids reported so far, that is, grafting with electron-rich multifunctional groups on the unsaturated Cr(III) sites. The amine-grafted MIL-101 exhibited remarkably high activities in the base-catalyzed reaction and, moreover, behaved as a size-selective molecular sieve catalyst according to the size of substrates and products. We have also succeeded in encapsulating noble metals such as Pd, Pt, and Au in the amine-grafted MIL-101. Among them, the Pd-loaded MIL-101 has been able to be used as a catalyst for the Heck coupling reaction. The present approach indeed ensures the development of newly functionalized catalysts for the immobilization and encapsulation of organic molecules and metal components. The essential concept to extend the strategy of surface functionalization will open up the development of versatile hybrid materials with new functions.

9. Experimental

MIL-101 was initially prepared from hydrothermal reaction of terephthalic acid (1 mmol) with $Cr(NO_3)_3{\cdot}9H_2O$ (1 mmol), HF, and H_2O (265 mmol) at 493 K for 8 h. In the synthesis, concentration of HF was varied in the range of 1–0.25 mmol. These reactions produced a highly crystallized green powder of the chromium terephthalate with formula $Cr_3Fx(H_2O)_2O[(O_2C)\text{-}C_6H_4\text{-}(CO_2)]_3{\cdot}nH_2O$ (where n is ≈25), based on chemical analysis. To obtain the pure crystals, the as-synthesized MIL-101 was further purified by the following two-step processes using hot ethanol and aqueous NH_4F solutions. Residual terephthalic acid in the as-synthesized MIL-101 (denoted MIL-101A), obtained from the double filtration can be effectively removed by subsequent solution treatments. A first activation treatment was performed using two subsequent solvent treatments such as boiling water at 70 °C for 5 h and hot ethanol at 60 °C for 3 h until no detection of colored impurities in the mother liquor solution, resulting in the more purified MIL-101 (denoted MIL-101B). The further purified solid denoted MIL-101C was obtained starting from MIL-101B (1 g) dispersed in 150 mL of an aqueous solution of 30 mM NH_4F at 60 °C for 10 h. After cooling, the precipitate was filtered and washed five times with 200 mL of hot water (60 °C) to remove traces of NH_4F. The hydrothermal stability of MIL-101 was investigated by mixing ≈0.2 g of the fresh MIL-101B sample with 50 g deionized water and heating in a closed bottle at 100 °C under static conditions for different time periods (up to 7 days).

The structure and crystallinity of the synthesized samples were determined by X-ray diffraction analysis (Rigaku, D/MAX IIIB, Cu Kα radiation). The BET surface area measurements were performed with N_2 adsorption-desorption isotherms at liquid nitrogen temperature (77 K) after dehydration under vacuum at 423 K for 12h using Micromeritics Tristar 3000. The specific surface areas were evaluated using the BET method in the p/p_0 range 0.05–0.3. Pore size distribution curves were calculated using the adsorption branch of the isotherms and the BJH method, and pore sizes were obtained from the peak positions of the distribution curves. The pore volume was taken by a single point method at $p/p_0 = 0.99$.

Acknowledgements

This work was supported by ISTK through the Institutional Research Program (grant no. KK-0904-A1). The authors thank Prof. S. H. Jhung, Prof. J. Kim, Prof. M. Daturi, Dr. A. Vimont, and Prof. P. L. Llewellyn for their helpful discussion and contribution, and CCME members for synthesis, grafting, catalysis, and adsorption experiments. This article appears as part of a special issue on materials science in Korea.

Received: August 2, 2008
Revised: October 23, 2008
Published online: April 20, 2009

[1] A. Corma, *Chem. Rev.* **1997**, *97*, 2373.
[2] M. E. Davis, *Chem. Eur. J.* **1997**, *3*, 1745.
[3] J. M. Thomas, *Scientific American* **1992**, *266*, 112.
[4] F. Schüth, W. Schmidt, *Adv. Mater.* **2002**, *14*, 629.
[5] A. K. Cheetham, G. Férey, T. Loiseau, *Angew. Chem. Int. Ed.* **1999**, *38*, 3268.
[6] S. T. Wilson, B. M. Lok, C. A. Messina, T. R. Cannan, E. M. Flanigen, *J. Am. Chem. Soc.* **1982**, *104*, 1146.
[7] G. Férey, A. K. Cheetham, *Science* **1999**, *283*, 1125.
[8] C. N. R. Rao, S. Natarajan, S. Neeraj, *J. Am. Chem. Soc.* **2000**, *122*, 2810.
[9] C. N. R. Rao, S. Natarajan, A. Choudhury, S. Neeraj, A. A. Ayi, *Acc. Chem. Res.* **2001**, *34*, 80.
[10] M. E. Davis, *Nature* **2002**, *417*, 81.
[11] P. Feng, X. Bu, G. D. Stucky, *Nature* **1997**, *388*, 735.
[12] N. Guillou, Q. Gao, P. M. Forster, J.-S. Chang, M. Nogues, S.-E. Park, G. Férey, A. K. Cheetham, *Angew. Chem. Int. Ed.* **2001**, *40*, 2831.
[13] J.-S. Chang, J.-S. Hwang, S. H. Jhung, S.-E. Park, G. Férey, A. K. Cheetham, *Angew. Chem. Int. Ed.* **2004**, *43*, 2819.
[14] G. Férey, *Chem. Soc. Rev.* **2008**, *37*, 191 and references therein.
[15] H. Li, M. Eddaoudi, M. O'Keefe, O. M. Yaghi, *Nature* **1999**, *402*, 276.
[16] S. Kitagawa, R. Matsuda, *Coord. Chem. Rev.* **2007**, *251*, 2490.
[17] A. K. Cheetham, C. N. R. Rao, R. K. Feller, *Chem. Commun.* **2006**, 4780.
[18] O. M. Yaghi, M. O'Keeffe, N. W. Ockwig, H. K. Chae, M. Eddaoudi, J. Kim, *Nature* **2003**, *423*, 705.
[19] S. L. James, *Chem. Soc. Rev.* **2003**, *32*, 276.
[20] X. Zhao, B. Xiao, A. Fletcher, K. M. Thomas, D. Bradshaw, M. J. Rosseinsky, *Science* **2004**, *306*, 1012.
[21] G. Férey, M. Latroche, C. Serre, F. Millange, T. Loiseau, A. Percheron-Guégan, *Chem. Commun.* **2003**, 2976.
[22] B. Panella, M. Hirscher, H. Pütter, U. Müller, *Adv. Funct. Mater.* **2006**, *16*, 520.
[23] M. Dincl, J. R. Long, *J. Am. Chem. Soc.* **2005**, *127*, 9376.
[24] B. Chen, N. W. Ockwig, A. R. Millward, D. S. Contreras, O. M. Yaghi, *Angew. Chem. Int. Ed.* **2005**, *44*, 4745.
[25] J. L. C. Rowsell, E. C. Spencer, J. Eckert, J. A. K. Howard, O. M. Yaghi, *Science* **2005**, *309*, 1350.
[26] B. Kesanli, Y. Cui, M. R. Smith, E. W. Bittner, B. C. Bockrath, W. Lin, *Angew. Chem. Int. Ed.* **2005**, *44*, 72.
[27] P. Pan, M. B. Sander, X. Huang, J. Li, M. Smith, E. Bittner, B. Bockrath, J. K. Johnson, *J. Am. Chem. Soc.* **2004**, *126*, 1308.
[28] S. Ma, D. Sun, J. M. Simmons, C. D. Collier, D. Yuan, H.-C. Zhou, *J. Am. Chem. Soc.* **2008**, *130*, 1012.
[29] M. Latroche, S. Surblé, C. Serre, C. Mellot-Draznieks, P. L. Llewellyn, J.-H. Lee, J.-S. Chang, S. H. Jhung, G. Férey, *Angew. Chem. Int. Ed.* **2006**, *45*, 8227.
[30] R. Kitaura, K. Seki, G. Akiyama, S. Kitagawa, *Angew. Chem. Intl. Ed.* **2003**, *42*, 428.
[31] S. Ma, D. Sun, X.-S. Wang, H.-C. Zhou, *Angew. Chem. Intl. Ed.* **2007**, *46*, 2458.
[32] J. S. Seo, D. Whang, H. Lee, S. I. Jun, J. Oh, Y. J. Jeon, K. Kim, *Nature* **2000**, *404*, 982.
[33] L.-G. Qiu, A.-J. Xie, L.-D. Zhang, *Adv. Mater.* **2005**, *17*, 689.
[34] P. M. Forster, A. K. Cheetham, *Top. Catal.* **2003**, *24*, 79.
[35] L. Alaerts, E. Séguin, H. Poelman, F. Thibault-Starzyk, P. A. Jacobs, D. E. De Vos, *Chem. Eur. J.* **2006**, *12*, 7353.
[36] R.-Q. Zou, H. Sakurai, Q. Zu, *Angew. Chem. Int. Ed.* **2006**, *45*, 2542.
[37] P. Horcajada, S. Surblé, C. Serre, D.-Y. Hong, Y.-K. Seo, J.-S. Chang, J.-M. Grenèche, I. Margiolaki, G. Férey, *Chem. Commun.* **2007**, 2820.
[38] P. Horcajada, C. Serre, M. Vallet-Regí, M. Sebban, F. Taulelle, G. Férey, *Angew. Chem. Int. Ed.* **2006**, *45*, 5974.
[39] P. Horcajada, C. Serre, G. Maurin, N. A. Ramsahye, F. Balas, M. Vallet-Regí, M. Sebban, F. Taulelle, G. Férey, *J. Am. Chem. Soc.* **2008**, *130*, 6774.
[40] B. Chen, Y. Yang, F. Zapata, G. Lin, G. Qian, E. B. Lobkovsky, *Adv. Mater.* **2007**, *19*, 1693.
[41] D. T. De Lill, N. S. Gunning, C. L. Cahill, *Inorg. Chem.* **2005**, *44*, 258.
[42] F. Pellé, S. Surblé, C. Serre, F. Millange, G. Férey, *J. Lumin.* **2007**, *122–123*, 492.
[43] B. V. Harbuzaru, A. Corma, F. Rey, P. Atienzar, J. L. Jordá, H. García, D. Ananias, L. D. Carlos, J. Rocha, *Angew. Chem. Int. Ed.* **2008**, *47*, 1080.
[44] D. Maspoch, D. Ruiz-Molina, J. Veciana, *J. Mater. Chem.* **2004**, *14*, 2713.
[45] S. M. Humphrey, T. J. P. Angliss, M. Aransay, D. Cavea, L. A. Gerrard, G. F. Weldona, P. T. Wood, *Z. Anorg. Allg. Chem.* **2007**, *633*, 2342.
[46] G. Férey, F. Millange, O. Morerette, J. M. Grenèche, M. L. Doublet, J. M. Tarascon, *Angew. Chem. Int. Ed.* **2007**, *46*, 1.
[47] C. Mellot-Draznieks, G. Ferey, *Prog. Solid State Chem.* **2006**, *33*, 187.
[48] S. Kitagawa, K. Uemura, *Chem. Soc. Rev.* **2005**, *34*, 109.
[49] K. Sanderson, *Nature* **2007**, *448*, 746.
[50] A. K. Cheetham, C. N. R. Rao, *Science* **2007**, *318*, 58.
[51] G. Férey, C. Mellot-Draznieks, C. Serre, F. Millange, *Acc. Chem. Res.* **2005**, *38*, 217.

[52] G. Férey, C. Mellot-Draznieckes, C. Serre, F. Millange, J. Dutour, S. Surblé, I. Margiolaki, *Science* **2005**, *309*, 2040.
[53] Y. K. Hwang, D.-Y. Hong, J.-S. Chang, S. H. Jhung, Y.-K. Seo, J. Kim, A. Vimont, M. Daturi, C. Serre, G. Férey, *Angew. Chem. Int. Ed.* **2008**, *47*, 4144.
[54] F. Schröder, D. Esken, M. Cokoja, M. W. E. van den Berg, O. L. Lebedev, G. V. Tendeloo, B. Walaszek, G. Buntkowsky, H.-H. Limbach, B. Chaudret, R. A. Fischer, *J. Am. Chem. Soc.* **2008**, *130*, 6119.
[55] G. Férey, *J. Solid State Chem.* **2000**, *152*, 37.
[56] C. Serre, F. Millange, S. Surblé, G. Férey, *Angew. Chem. Intl. Ed.* **2004**, *43*, 6285.
[57] G. Férey, C. Serre, C. Mellot-Draznieckes, F. Millange, Julien. Dutour, S. Surblé, I. Margiolaki, *Angew. Chem. Int. Ed.* **2004**, *43*, 6296.
[58] Collection of Simulated XRD Powder Patterns for Zeolites (Eds: M. M. J. Tracy, J. B. Higgins), Elsevier, Amsterdam, Netherlands **2007**, p. 296.
[59] O. I. Lebedev, F. Millange, C. Serre, G. Van Tendeloo, G. Férey, *Chem. Mater.* **2005**, *17*, 6525.
[60] U. Mueller, M. Schuber, F. Teich, H. Puetter, K. Schierle-Arndt, J. Pastré, *J. Mater. Chem.* **2006**, *16*, 626.
[61] S. H. Jhung, J.-H. Lee, J. W. Yoon, C. Serre, G. Férey, J.-S. Chang, *Adv. Mater.* **2007**, *19*, 121.
[62] S. H. Jhung, J.-H. Lee, P. M. Forster, G. Férey, A. K. Cheetham, J.-S. Chang, *Chem. Eur. J.* **2006**, *12*, 899.
[63] Y. K. Hwang, J.-S. Chang, S.-E. Park, D. S. Kim, Y.-U. Kwon, S. H. Jhung, J.-S. Hwang, M.-S. Park, *Angew. Chem, Intl. Ed.* **2005**, *44*, 557.
[64] S.-E. Park, J.-S. Chang, Y. K. Hwang, D. S. Kim, S. H. Jhung, J.-S. Hwang, *Catal. Survey Asia* **2004**, *8*, 91.
[65] D. P. Amalnerkar, H.-Y. Lee, Y. K. Hwang, D.-P. Kim, J.-S. Chang, *J. Nanosci. Nanotechnol.* **2007**, *7*, 4412.
[66] Z. Lin, D. S. Wragg, R. E. Morris, *Chem. Commun.* **2006**, 2021.
[67] N. Stock, T. Bein, *Angew. Chem. Int. Ed.* **2004**, *43*, 749.
[68] E. R. Parnham, R. E. Morris, *Acc. Chem. Res.* **2007**, *40*, 1005.
[69] C. Serre, J. A. Groves, P. Lightfood, A. M. Z. Slawin, P. A. Wright, N. Stock, T. Bein, M. Haouas, F. Taulelle, G. Férey, *Chem. Mater.* **2006**, *18*, 1451.
[70] P. M. Forster, A. R. Burbank, C. Livage, G. Férey, A. K. Cheetham, *Chem. Commun.* **2004**, 368.
[71] P. M. Forster, N. Stock, A. K. Cheetham, *Angew. Chem. Int. Ed.* **2005**, *44*, 7608.
[72] T. Loiseau, G. Férey, *J. Fluorine Chem.* **2007**, *128*, 413.
[73] D. S. Kim, J.-S. Chang, J. S. Hwang, S.-E. Park, J. M. Kim, *Micrporous Mesoporous Mater.* **2004**, *68*, 77.
[74] S. H. Jhung, J.-S. Chang, Y. K. Hwang, S.-E. Park, *J. Mater. Chem.* **2004**, *14*, 280.
[75] G. Tompsett, W. C. Conner, K. S. Yngvesson, *ChemPhysChem.* **2006**, *7*, 296.
[76] Y. K. Hwang, J.-S. Chang, Y.-U. Kwon, S.-E. Park, *Microporous Meosporous Mater.* **2004**, *68*, 21.
[77] M. Park, S. Komarneni, *Microporous Meosporous. Mater.* **1998**, *20*, 39.
[78] Z. Ni, R. I. Masel, *J. Am. Chem. Soc.* **2006**, *128*, 12394.
[79] S. H. Jhung, J.-H. Lee, H.-S. Chang, *Bull. Kor. Chem. Soc.* **2005**, *26*, 880.
[80] J. Y. Choi, J. Kim, S. H. Jhung, H.-K. Kim, J.-S. Chang, H. K. Chae, *Bull. Kor. Chem. Soc.* **2006**, *27*, 1523.
[81] E. Biemmi, C. Scherb, T. Bein, *J. Am. Chem. Soc.* **2007**, *129*, 8054.
[82] V. N. Soloviev, A. Eichhofer, D. Fenske, U. Banin, *J. Am. Chem. Soc.* **2001**, *123*, 2354.
[83] O. M. Yaghi, M. O'Keeffe, N. W. Ockwig, H. K. Cahe, M. Eddaoudi, J. Kim, *Nature* **2003**, *423*, 705.
[84] W. C. Conner, G. Tompsett, K.-H. Lee, K. S. Yngvesson, *J. Phys. Chem. B* **2004**, *108*, 13913.
[85] O. K. Farha, K. L. Mulfort, A. M. Thorsness, J. T. Hupp, *J. Am. Chem. Soc.* **2008**, *130*, 8598.
[86] L. Alaerts, M. Maes, P. A. Jacobs, J. F. M. Denayer, D. E. De Vos, *Phys. Chem. Chem. Phys.* **, 10**, 2979.
[87] S. Ma, D. Sun, M. Ambrogio, J. A. Fillinger, S. Parkin, H.-C. Zhou, *J. Am. Chem. Soc.* **2007**, *129*, 1858.
[88] L. Huang, H. Wang, J. Chen, Z. Wang, J. Sun, D. Zhao, Y. Yan, *Microporous Mesoporous Mater.* **2003**, *58*, 105.
[89] J. Liu, J. T. Culp, S. Natesakhawat, B. C. Bockrath, B. Zande, S. G. Sankar, G. Garberoglio, J. K. Johnson, *J. Phys. Chem. C* **2007**, *111*, 9305.
[90] J. Hafizovic, M. Bjørgen, U. Olsvye, P. D. C. Dietzel, S. Bordiga, C. Prestipino, C. Lamberti, K. P. Lillerud, *J. Am. Chem. Soc.* **2007**, *129*, 3612.
[91] Q. M. Wang, D. M. Shen, M. Bulow, M. L. Lau, S. G. Deng, F. R. Fitch, N. O. Lemcoff, J. Semanscin, *Microporous Mesoporous Mater.* **2002**, *55*, 217.
[92] B. Xiao, P. S. Wheatley, X. B. Zhao, A. J. Fletcher, S. Fox, A. G. Rossi, S. Megson, S. Bordiga, L. Regli, K. M. Thomas, R. E. Morris, *J. Am. Chem. Soc.* **2007**, *129*, 1203.
[93] Y. Li, R. T. Yang, *AIChE J.* **2008**, *54*, 269.
[94] I. Senkovska, S. Kaskel, *Microporous Mesoporous Mater.* **2008**, *112*, 108.
[95] Y.-Y. Liu, J.-L. Zeng, J. Zhang, F. Xu, L.-X. Sun, *Int. J. Hydrogen Energy* **2007**, *32*, 4005.
[96] S. B. Choi, M. J. Seo, M. Cho, Y. Kim, M. K. Jin, D.-Y. Jung, J.-S. Choi, W.-S. Ahn, J. L. C. Rowsell, J. Kim, *Cryst. Growth Design* **2007**, *7*, 2290.
[97] N. V. Maksimchuk, M. N. Timofeeva, M. S. Melgunov, A. N. Shmakov, Yu, A. Chesalov, D. N. Dybtsev, V. P. Fedin, O. A. Khodeeva, *J. Catal.* **2008**, *257*, 315.
[98] S. Bourrelly, P. L. Llewellyn, C. Serre, A. Vimont, M. Daturi, L. Hamon, G. De Weireld, J.-S. Chang, D.-Y. Hong, Y. K. Hwang, G. Férey, *Langmuir* **2008**, *24*, 7245.
[99] K. Schlichte, T. Kratzke, S. Kaskel, *Microporous Mesoporous Mater.* **2004**, *73*, 81.
[100] Y. Li, R. T. Yang, *Langmuir* **2007**, *23*, 12937.
[101] B. Panella, M. Hirscher, *Adv. Mater.* **2005**, *17*, 538.
[102] R. Kikuchi, *Energy Environ.* **2003**, *14*, 383.
[103] A. R. Millward, O. M. Yaghi, *J. Am. Chem. Soc.* **2005**, *127*, 17998.
[104] Q. M. Wang, D. Shen, M. Bülow, M. L. Lau, S. Deng, F. R. Fitch, N. O. Lemcoff, J. Semanscin, *Microporous Mesoporous Mater.* **2002**, *55*, 217.
[105] J. A. Dunne, M. Rao, S. Sircar, R. J. Gorte, A. L. Myers, *Langmuir* **1996**, *12*, 5896.
[106] G. Maurin, S. Bourrelly, P. L. Llewellyn, R. G. Bell, *Microporous Mesoporous Mater.* **2006**, *89*, 96.
[107] U. D. Joshi, P. N. Joshi, S. S. Tamhankar, V. V. Joshi, V. P. Shiralkar, *J. Catal.* **2001**, *235*, 135.
[108] A. Vimont, J.-M. Goupil, J.-C. Lavalley, Marco Daturi, S. Surblé, C. Serre, F. Millange, G. Férey, N. Audebrand, *J. Am. Chem. Soc.* **2006**, *128*, 3218.
[109] M. Dincl, J. R. Long, *J. Am. Chem. Soc.* **2007**, *129*, 1172.
[110] S. S.-Y. Chui, S. M.-F. Lo, J. P. H. Charmant, A. G. Prpen, I. D. Williams, *Science* **1999**, *283*, 1148.
[111] H. Li, C. E. Davis, T. L. Groy, D. G. Kelley, O. M. Yaghi, *J. Am. Chem. Soc.* **1998**, *120*, 2186.
[112] P. M. Forster, J. Eckert, B. D. Heiken, J. B. Parise, J. W. Yoon, S. H. Jhung, J.-S. Chang, A. K. Cheetham, *J. Am. Chem. Soc.* **2006**, *128*, 16846.
[113] B. Kesanli, W. Lin, *Coord. Chem. Soc.* **2003**, *246*, 305.
[114] S. Kitagawa, R. Kitaura, S.-I. Noro, *Angew. Chem. Int. Ed.* **2004**, *43*, 2334.
[115] S. Kitagawa, S.-I. Noro, T. Nakamura, *Chem. Commun.* **2006**, 701.
[116] S. Hasegawa, S. Horike, R. Matsuda, S. Furukawa, K. Mochizuki, Y. Kinoshita, S. Kitagawa, *J. Am. Chem. Soc.* **2007**, *129*, 2607.
[117] Z. Wang, S. M. Cohen, *J. Am. Chem. Soc.* **2007**, *129*, 12368.
[118] Y.-F. Song, L. Cronin, *Angew. Chem. Int. Ed.* **2008**, *47*, 4635.
[119] A. P. Wight, M. E. Davis, *Chem. Rev.* **2002**, *102*, 3589.
[120] A. Sayari, S. Hamoudi, *Chem. Mater.* **2001**, *13*, 3151.
[121] S. Huh, H.-T. Chen, J. W. Wiench, M. Pruski, V. S.-Y. Lin, *Angew. Chem. Int. Ed.* **2005**, *44*, 1826.
[122] M. W. McKittrick, C. W. Jones, *Chem. Mater.* **2003**, *15*, 1132.
[123] X. Wang, X. Tseng, Y. Chan, J. C. C. Cheng, *J. Catal.* **2005**, *233*, 266.
[124] D. A. Young, T. B. Freedman, E. D. Lipp, L. A. Nafie, *J. Am. Chem. Soc.* **1986**, *108*, 7255.
[125] J. A. Melero, R. van Grieken, G. Morales, *Chem. Rev.* **2006**, *106*, 3790.
[126] M. Műller, S. Hermes, K. Kähler, M. W. E. Van den Berg, M. Muhler, R. A. Fischer, *Chem. Mater.* **2008**, *20*, 4576.

[127] S. Hermes, M.-K. Schröder, R. Schmid, L. Knodeir, M. Muhler, A. Tissler, R. W. Fischer, R. A. Fischer, *Angew. Chem. Int. Ed.* **2005**, *44*, 1261.
[128] H. R. Moon, J. H. Kim, M. Paik Suh, *Angew. Chem. Int. Ed.* **2005**, *44*, 1261.
[129] M. Sabo, A. Henschel, H. Froede, E. Klemm, S. Kaskel, *J. Mater. Chem.* **2007**, *17*, 3827.
[130] P. Horcajada, C. Serre, M. Vallet-Regi, M. Sebban, F. Taulelle, G. Férey, *Angew. Chem. Int. Ed.* **2006**, *45*, 5974.
[131] C.-D. Wu, W. Lin, *Angew. Chem. Int. Ed.* **2007**, *46*, 1075.
[132] L. Alaerts, E. Séguin, H. Poelman, F. Thibault-Starzyk, P. A. Jacobs, D. E. De Vos, *Chem. Eur. J.* **2006**, *12*, 7353.
[133] Y. K. Hwang, D.-Y. Hong, J.-S. Chang, H. Seo, J. Kim, S. H. Jhung, C. Serre, G. Férey, Appl. Catal. A: Ger. **2009**, in press.
[134] M. Schenk, B. Smit, T. J. H. Vlugt, T. L. M. Masesen, *Angew. Chem. Int. Ed.* **2001**, *40*, 736.
[135] L. Yin, J. Liebscher, *Chem. Rev.* **2007**, *107*, 133.